Author Manuscript

Author Manuscript

Author Manuscript

Author Manuscript

HHS Public Access

Author manuscript

Mol Pharm. Author manuscript; available in PMC 2020 January 07.

Published in final edited form as:

Mol Pharm. 2019 January 07; 16(1): 214–226. doi:10.1021/acs.molpharmaceut.8b00951.

Labeling Single Domain Antibody Fragments with Fluorine-18 Using 2,3,5,6-Tetrafluorophenyl 6-[^{18}F]Fluoronicotinate Resulting in High Tumor to Kidney Ratios

Zhengyuan Zhou, **Darryl McDougald**, **Nick Devoogdt**, **Michael R. Zalutsky**, and **Ganesan Vaidyanathan**[*]

Department of Radiology, Duke University Medical Center, Durham, North Carolina 27710, USA

Abstract

ImmunoPET agents are being investigated to assess the status of epidermal growth factor receptor 2 (HER2) in breast cancer patients with the goal of selecting those likely to benefit from HER2-targeted therapies and monitoring their progress after these treatments. We have been exploring the use of single domain antibody fragments (sdAbs) labeled with ^{18}F using residualizing prosthetic agents for this purpose. In this study, we have labeled two sdAbs that bind to different domains on the HER2 receptor — 2Rs15d and 5F7 — using 2,3,5,6-tetrafluorophenyl 6-[^{18}F]fluoronicotinate ([^{18}F]TFPFN) and evaluated their HER2 targeting properties in vitro and in vivo. The overall decay-corrected radiochemical yield for the synthesis of [^{18}F]TFPFN-2Rs15d and [^{18}F]TFPFN-5F7 was 5.7 ± 3.6% and 4.0 ± 2.0%, respectively. Radiochemical purity of labeled sdAbs was >95%; immunoreactive fractions were about 60% and affinity was in the low nanomolar range. Intracellularly trapped activity from [^{18}F]TFPFN-2Rs15d and [^{18}F]TFPFN-5F7 in HER2-expressing SKOV-3 ovarian and BT474M1 breast carcinoma cells were similar to the sdAbs labeled using the previously validated radioiodination residualizing prosthetic agents *N*-succinimidyl 4-guanidinomethyl-3-[^{125}I]iodobenzoate ([^{125}I]SGMIB) and *N*-succinimidyl 3-guanidinomethyl-5-[^{125}I]iodobenzoate (*iso*-[^{125}I]SGMIB). Intracellular activity was about 2-fold higher for radiolabeled 5F7 compared with 2Rs15d for both ^{18}F and ^{125}I. While tumor uptake of both [^{18}F]TFPFN-2Rs15d and [^{18}F]TFPFN-5F7 was comparable to those for the co-administered ^{125}I-labeled sdAb, renal uptake of the ^{18}F-labeled sdAbs was substantially lower. In microPET images, tumor was clearly delineated in SKOV-3 and BT474 xenograft-bearing athymic mice with low levels of background activity in normal tissues except bladder. These results indicate that the [^{18}F]TFPFN prosthetic group could be a valuable reagent for developing sdAb-based immunoPET imaging agents.

Table of Contents Graphic

[*]Corresponding Author: Ganesan Vaidyanathan, Ph.D., 161C, Bryan Research Building, 311 Research Drive, Durham, North Carolina 27710, USA. Tel.: (919) 684-7811; ganesan.v@duke.edu.

Author Manuscript Author Manuscript Author Manuscript Author Manuscript

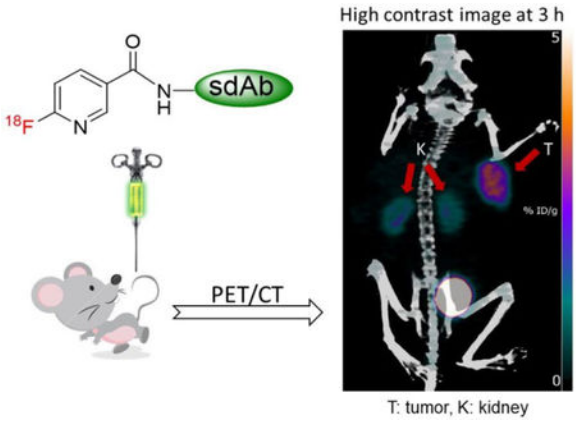

Keywords

HER2; single domain antibody fragment; fluorine-18; N-Succinimidyl 4-fluorobenzoate (SFB); 2,3,5,6-etrafluorophenyl 6-fluoronicotinate (TFPFN); immunoPET

INTRODUCTION

Given that only about 20–25% of breast cancer patients have tumor that express the receptor tyrosine kinase HER2, it is important to determine tumor HER2 levels before administering HER2-targeted therapies.[1, 2] This has spurred great interest in the development of radiolabeled probes for the noninvasive assessment of HER2 levels by PET imaging to stratify patients for HER2-targeted therapy and to evaluate therapeutic response. Indeed, many vectors such as affibodies, single chain antibody fragments, and diabodies as well as intact antibodies have been labeled with different positron emitters with the goal of assessing HER2 levels by PET.[3–6]

Single domain antibody fragments (sdAbs; a.k.a. V_HH or Nanobody®) are the smallest naturally occurring antigen binding fragments that are derived from the heavy-chain-only antibodies produced by Camelids.[7, 8] Properties that make them attractive as a scaffold for developing imaging agents are their high stability, low immunogenicity and ability to bind to their molecular targets with nanomolar affinity and high specificity. Because of their small size (12–15 kDa), they penetrate tumor tissues better than intact antibodies. Furthermore, this property allows them to clear faster from the blood, making them ideal for labeling with the short-lived and widely available positron emitters ^{18}F and ^{68}Ga. For these reasons, radiolabeled sdAbs are being investigated extensively for diagnostic and therapeutic purposes.[9–15]

Although there are several positron-emitting radionuclides available, ^{18}F is the most versatile among these because of its ideal physical properties and ready availability.[16, 17] Not surprisingly, a variety of prosthetic agents and approaches has been developed for labeling peptides and proteins with ^{18}F.[18–21] Nonetheless, *N*-succinimidyl 4-[^{18}F]fluorobenzoate ([^{18}F]SFB), an agent that we developed more than 25 years ago,[22] remains the most commonly used prosthetic agent for ^{18}F labeling. Following the success obtained with

Author Manuscript Author Manuscript Author Manuscript Author Manuscript

residualizing labels for labeling internalizing biomolecules with radioiodine and ^{211}At,[14, 23] we have been pursuing a similar strategy for ^{18}F labeling.[24, 25] Although higher tumor uptake was obtained when an anti-HER2 sdAb 5F7 was labeled with ^{18}F using the residualizing agent, *N*-succinimidyl 3-((4-(4-[^{18}F]fluorobutyl)-1*H*-1,2,3-triazol-1-yl)methyl)-5-(guanidinomethyl)benzoate ([^{18}F]SFBTMGMB; [^{18}F]RL-I) compared with [^{18}F]SFB, considerably higher renal uptake was also seen with this new prosthetic agent.[24]

The archetypal prosthetic agent for radioiodination for use with non-internalizing molecules is *N*-succinimidyl 3-[*I]iodobenzoate ([*I]SIB).[26] Hypothesizing that the presence of a positively charged moiety would increase trapping of activity within tumor cells, a second generation agent was developed by replacing the benzene ring in [*I]SIB with a pyridine ring yielding *N*-succinimidyl 5-[*I]iodo-3-pyridinecarboxylate ([*I]SIPC).[27] Indeed, when the internalizing anti-EGFRvIII antibody L8A4 was radioiodinated using [*I]SIPC, higher activity levels of radioiodine were trapped in tumor cells both in vitro and in vivo; however, the advantage was transient.[28] Given the short half-life of ^{18}F, the unprolonged duration of this enhanced trapping in tumor might not be a significant limitation, providing motivation for the current study in which we evaluated an analogous pyridine-containing agent for labeling sdAbs with ^{18}F. Based on our previous work with the analogous iodinated compound,[27] we hypothesized that this strategy would result in higher tumor uptake and lower activity in the kidneys than seen with [^{18}F]SFB labeling.

While a prosthetic agent analogous to SIPC for ^{18}F-labeling (*N*-succinimidyl 6-[^{18}F]fluoronicotinate; [^{18}F]SFN) has been reported in a patent literature,[29] to our knowledge, no work related to this molecule has been published. On the other hand, the synthesis of 2,3,5,6-tetrafluorophenyl 6-[^{18}F]fluoronicotinate ([^{18}F]TFPFN) and its usefulness in labeling an RGD peptide has been reported by Olberg et al.[30] Moreover, a simple, on-cartridge synthesis of [^{18}F]TFPFN that does not require the customary drying of [^{18}F]fluoride was recently reported.[31, 32]

In the current study, we first attempted to label the anti-HER2 sdAb 2Rs15d with ^{18}F using [^{18}F]SFN; however, conjugation yields were not satisfactory. Subsequently, we labeled 2Rs15d using [^{18}F]TFPFN, which in turn was synthesized using the on-cartridge method. Another anti-HER2 sdAb, 5F7, which undergoes more extensive internalization,[25, 33] was also labeled using [^{18}F]TFPFN. The ^{18}F-labeled sdAbs [^{18}F]TFPFN-2Rs15d and [^{18}F]TFPFN-5F7 were evaluated, in comparison to 2Rs15d radioiodinated using *N*-succinimidyl 4-guanidinomethyl-3-[^{125}I]iodobenzoate ([^{125}I]SGMIB) — the prototypical radioiodination residualizing label[34] — or its isomeric version (*iso*-[^{125}I]SGMIB-5F7), which we have recently shown to be the better isomer for 5F7 labeling,[35] respectively. Studies were performed on HER2-expressing SKOV-3 ovarian carcinoma and BT474 breast carcinoma cells in vitro and in athymic mice bearing subcutaneous xenografts derived from these cell lines in vivo. In addition, microPET/CT imaging was performed after administration of [^{18}F]TFPFN-2Rs15d and [^{18}F]TFPFN-5F7 in these xenograft models.

Author Manuscript Author Manuscript Author Manuscript Author Manuscript

EXPERIMENTAL SECTION

General.

All reagents were purchased from Sigma-Aldrich except where noted. Sodium [^{125}I]iodide (81.4 TBq/mmol) in 0.1 N NaOH was obtained from Perkin-Elmer Life and Analytical Sciences (Boston, MA). Fluorine-18 was obtained either by in-house cyclotron irradiation of [^{18}O]H_2O as described before[36] or from PET-NET solutions (Durham, NC). Synthesis of [^{125}I]SGMIB and *iso*-[^{125}I]SGMIB, and sdAb radioiodination using them were performed as reported before.[14, 34, 36, 37] *N,N,N*-trimethyl-5-((2,3,5,6-tetrafluorophenoxy)carbonyl)pyridin-2-aminium trifluoromethane sulfonate (**2**) was synthesized following a known procedure.[30] The anti-HER2 antibody, trastuzumab (Roche/Genentech) was obtained from the Duke University Medical Center Pharmacy. Normal phase column chromatography was performed with the Biotage Isolera chromatography system (Charlotte, NC) using their prepacked columns. High performance liquid chromatography (HPLC) was conducted using two Agilent 1260 Infinity systems equipped with a 1260 Infinity Multiple Wavelength Detector (Santa Clara, CA). For monitoring radioactivity, one system was connected to a Dual Scan-RAM flow activity detector/TLC scanner and the other to a Flow-RAM detector (Lablogic, Tampa, Florida); both the HPLC and the gamma detectors were controlled by LabLogic Laura® software. Size-exclusion HPLC was performed using a TSKgel Super SW2000 4.6 mm × 30 cm column attached to a 4.6 × 3.5 cm guard column (Tosoh Bioscience, Montgomeryville, PA). This column was equilibrated and eluted in isocratic mode with PBS, pH 7.0, at a flow rate of 0.3 mL/min with a run time of 25 min. Chromafix® 30-PS-HCO_3 anion-exchange cartridges were purchased from ABX Advanced Biochemical Compounds (Radeberg, Germany). They were conditioned by sequential passage of 1.0 mL ethanol and 1.0 mL deionized water. Oasis MCX Plus cartridges, obtained from Waters, were conditioned by elution with 5 mL ethanol, drying with 10 mL air and then passage of 10 mL water. Disposable PD 10 desalting columns for gel filtration were purchased from GE Healthcare (Piscataway, NJ). Radioctivity in various samples was measured using a CRC-7 dose calibrator (Capintec, Pittsburgh, PA) for higher activity levels, and either an LKB 1282 (Wallac, Finland) or a Perkin Elmer Wizard II (Shelton, CT) automated gamma counter for lower activity levels. Proton NMR spectra of samples were obtained on a 400 MHz spectrometer (Varian/Agilent; Inova) and chemical shifts are reported in units using the residual solvent peaks as a reference. Mass spectra were obtained using an Advion (Ithaca, NY) Expression^L CMS LC-MS System attached to an Agilent 1260 infinity HPLC like the system described above. This mass spectrometer has the capability of determining molecular weights of compounds directly from TLC plates (Plate Express) and by ESI, APCI, and ASAP.

Single domain antibodies, cells culture conditions and the animal model.

Details of production, purification and characterization of anti-HER2 sdAb 2Rs15d have been reported previously.[38, 39] Another anti-HER2 sdAb 5F7 was obtained as a gift from Dr. Hilde Revets formerly of Ablynx NV (Ghent, Belgium). This anti-HER2 sdAb was selected from phage libraries derived from *llamas* immunized with SKBR-3 human breast carcinoma cells, and details for its production, purification and characterization have been described

Author Manuscript Author Manuscript Author Manuscript Author Manuscript

previously.[40] Both sdAbs were devoid of His-tags or GGC tails and were present exclusively as monomers.

Cell culture reagents were purchased from Thermo Fisher Scientific (Waltham, MA) except where noted. SKOV-3 human ovarian carcinoma cells and BT474 human breast carcinoma cells were obtained from Duke University Cell Culture Facility. SKOV-3 cells were grown in McCoy's 5A medium containing 10% fetal bovine serum and 1% penicillin-streptomycin; BT474 cells in DMEM/F12 media, containing 10% fetal bovine serum and 1% penicillin-streptomycin. Cells from more tumorigenic, metastatic subclone of BT474, designated as BT474M1[41, 42] were provided by Dr. Kim Lyerly, Duke University Medical Center. These cells were grown in DMEM-HG media containing 10% fetal bovine serum, 1% penicillin-streptomycin and Ciprofloxacin 10 μg/mL. Cells were cultured at 37ºC in a 5% CO_2 humidified incubator. All experiments involving animals were performed under a protocol approved by the Duke University IACUC. Subcutaneous SKOV-3 xenografts were established by inoculating 10-week old female athymic nude mice (obtained from a colony maintained by the Duke University Division of Laboratory Animal Resources) with 5×10^6 SKOV-3 cells in 50% Matrigel (Corning Inc. NY) in the above medium (100 μL) in the shoulder. The tumors were allowed to grow until they reached a volume of 350–500 mm^3 (~5–6 weeks). BT474 xenografts in athymic nude mice were established as reported before.[43, 44] Briefly, 10-week old female athymic nude mice were implanted between the shoulder blades with 60-day release estrogen pellets (0.72 mg estradiol; Innovative Research of America, Sarasota, FL). Two to three days later, 5×10^6 BT474 cells in 50% Matrigel in the above medium (100 μL) were subcutaneously inoculated in the shoulder. Biodistribution and microPET/CT imaging studies were performed 6–8 wk later, when tumors reached 350–500 mm^3 in size.

Chemistry.

2,3,5,6-Tetrafluorophenyl 6-fluoronicotinate[30] (*1*).—Dicyclohexylcarbodiimide (110 mg; 0.53 mmol) was added to a solution of 6-fluoronicotinic acid (50 mg; 0.35 mmol) and 2,3,5,6-tetrafluorophenol (88 mg; 0.53 mmol) in 20 mL of dichloromethane, and the mixture stirred at 20°C for 16 h. The precipitated dicyclohexyl urea was filtered off, and the filtrate was washed with water. After drying the organic layer with anhydrous sodium sulfate, dichloromethane was evaporated. The crude product was purified by preparative TLC using 1:1 hexanes:ethyl acetate as the mobile phase to afford 42 mg (41%) of **1** as a white solid: ^{1}H-NMR ($CDCl_3$) δ 9.07 (s, 1H), 8.55 (d, 1H; J=8.0), 7.13–7.04 (m, 1H), 6.58–6.50 (m, 1H). LRMS (LCMS-ESI-negative mode) m/z: 288 $(M-H)^-$.

Radiochemistry.

2,3,5,6-Tetrafluorophenyl 6-[^{18}F]fluoronicotinate ([^{18}F]1).—This was synthesized essentially following the procedure reported.[31, 32] Briefly, an aqueous solution of ^{18}F (1.85 – 5.55 GBq; ~1 mL) was passed through a conditioned Chromafix® 30-PS-HCO_3 cartridge followed by 6 mL of ethanol. After drying the cartridge by flushing it with argon for 5 min, 2 × 0.5 mL of a solution of **2** in 1:4 (v/v) acetonitrile:*tert*-butanol (10 mg/mL) was slowly passed through the cartridge followed with 1 mL of acetonitrile. The entire eluate was passed through a conditioned Oasis MCX® plus cartridge and the cartridge was washed with

Author Manuscript Author Manuscript Author Manuscript Author Manuscript

5 mL of ether. The solvents from the eluate containing [^{18}F]**1** was evaporated to near dryness. The residual activity was taken up in 95:5 hexanes:ethyl acetate (0.1 mL), and injected onto the normal phase semi-preparative HPLC column (Agilent ZORBAX RX-SIL 5 μM 9.4 × 250 mm), which was eluted isocratically with 95:5 hexanes:ethyl acetate at a flow rate of 3 mL/min. The fractions containing [^{18}F]**1** (t_R = 9.1 min) were pooled and the solvents were evaporated with a gentle stream of argon.

Fluorine-18 labeling of sdAbs using [^{18}F]TFPFN.—This was performed essentially using the procedure reported previously for the conjugation of radiolabeled active esters with sdAbs.[25, 37] Briefly, to the dried activity of [^{18}F]**1** (0.08 – 1.52 GBq), a solution of sdAb in 0.1 M borate buffer, pH 8.5 (50 μL; 2 mg/mL) was added, and the mixture incubated at 20°C for 20 min. The labeled sdAb was isolated by gel filtration over a PD10 column using PBS as the mobile phase. Fractions containing the ^{18}F-labeled sdAb were pooled and used for studies described below.

Quality control evaluation of [^{18}F]TFPFN-2Rs15d and [^{18}F]TFPFN-5F7.—The radiochemical purity of labeled sdAbs was evaluated by TCA precipitation to determine total protein-associated activity, SDS-PAGE/phosphor imaging and by size-exclusion chromatography ([^{18}F]TFPFN-2Rs15d only) as reported previously for 2Rs15d labeled using another prosthetic agent.[25] The immunoreactive fraction of the [^{18}F]TFPFN-sdAb conjugates was determined by the Lindmo method[45] using magnetic beads coated with the extracellular domain of HER2 or, as a negative control, with HSA, prepared as described.[46] Briefly, aliquots of [^{18}F]TFPFN-sdAb (~5 ng) were incubated in duplicate with three or four doubling concentrations of both positive (HER2) and negative (HSA) beads. Reciprocals of the percentage of specific binding (positive minus negative) were plotted against the reciprocals of bead concentration; the immunoreactive fraction was calculated as the reciprocal of Y-intercept, which is specific binding at the infinite antigen concentration.[45]

The binding affinity of [^{18}F]TFPFN-sdAb conjugates to HER2 was determined by a saturation binding assay using both SKOV-3 and BT474M1 carcinoma cell lines. For this, cells were plated in 24-well plates at a density of 8×10^4 cells/well/mL and incubated overnight at 37°C. After allowing the cells to acclimatize at 4°C for 30 min, increasing concentrations of [^{18}F]TFPFN-sdAb (0.1–300 nM; 0.6 mL total volume per well) were added in triplicate. The cells were incubated at 4°C for 2 h, the medium containing unbound activity was removed, and the cells were washed twice with cold PBS. The cells were then solubilized by treatment with 0.5 mL of 0.1% SDS at 37°C for 10 min, and the cell-associated activity was measured using an automated gamma counter. Nonspecific binding was determined in parallel assays performed as above but by co-incubating cells with a 100-fold molar excess of 2Rs15d or, in the case of 5F7, trastuzumab. The data were fit using GraphPad Prism software to determine the K_d value.

Determination of internalization in vitro.—Internalization and cellular retention of [^{18}F]TFPFN-2Rs15d and [^{18}F]TFPFN-5F7 in tandem with [^{125}I]SGMIB-2Rs15d and *iso*-[^{125}I]SGMIB-5F7, respectively, in SKOV-3 and/or BT474M1 cells was assessed in a paired-label format as described for other radiolabeled sdAbs.[14, 25] Cells at a density of 8×10^5 cells per well in 3 mL medium were plated in six-well plates and incubated at 37°C

Author Manuscript Author Manuscript Author Manuscript Author Manuscript

overnight. The cells were brought to 4°C and incubated for 30 min, and the cold medium was replaced with 2 mL fresh medium at 4°C containing [^{18}F]TFPFN-2Rs15d and [^{125}I]SGMIB-2Rs15d, or [^{18}F]TFPFN-5F7 and *iso*-[^{125}I]SGMIB-5F7 (5 nM of each sdAb). After incubating the cells at 4°C for 1 h, cell culture supernatants containing unbound activity were collected, and 2 mL fresh medium at 37°C was added. The cells were incubated at 37°C for 1, 2, and 4 h and processed as follows: Cell culture supernatants were collected, and the cells were washed with an acidic buffer consisting of 50 mM glycine-HCl/0.1 M NaCl, pH 2.8, to strip off membrane-bound activity. Finally, the cells were lysed by incubation with 1 mL of 0.1 % SDS. Activity in cell lysates, acid washes, and cell culture supernatants was counted, and from these values, the percentage of activity initially bound to the cells that was present in cell culture supernatant, membrane-bound fraction (acid washes) and cell lysates was calculated. Nonspecific uptake was determined in a parallel experiment as above but with a 100-fold molar excess of 2Rs15d (for 2Rs15d) or trastuzumab (for 5F7) included in the incubation with the labeled sdAb preparations.

Biodistribution experiments.—The biodistribution of [^{18}F]TFPFN-2Rs15d and [^{125}I]SGMIB-2Rs15d was determined in a paired-label format in athymic mice bearing SKOV-3 xenografts. Groups of mice (1 h, n = 5; 2 and 3 h, n = 4) were injected intravenously with 0.15 – 0.19 MBq of [^{125}I]SGMIB-2Rs15d and 0.30 – 0.37 MBq of [^{18}F]TFPFN-2Rs15d. Unlabeled 2Rs15d was added such that each mouse received a total of 10 μg of 2Rs15d. In a second experiment, a group of four athymic mice bearing BT474 xenografts was injected intravenously with 0.07 MBq (1.33 μg) of *iso*-[^{125}I]SGMIB-5F7 and 0.93 MBq (0.5 μg) of [^{18}F]TFPFN-5F7, and biodistribution was performed at 2 h. At indicated time points, after collecting blood and urine, mice were killed, and their tissues harvested, blot-dried, weighed, and activity levels were determined using the gamma counter. Results were expressed as the percentage of the injected dose per gram tissue (%ID/g) and tumor-to-normal tissue ratios. Statistical significance of the differences observed for the uptake of the two matched radioconjugates was determined by a paired Student *t* test using the GraphPad prism program; a *P* value of <0.05 was considered to be significant.

MicroPET/CT imaging.—Imaging of both SKOV-3 and BT474 subcutaneous xenograft-bearing mice was performed on a Siemens Inveon microPET/CT system (Knoxville, TN). Imaging was performed with 3 mice bearing SKOV-3 xenografts 1 h, 2 h and 3 h after administration of 1.6– 2.5 MBq (2.2–3.2 μg) [^{18}F]TFPFN-2Rs15d. With [^{18}F]TFPFN-5F7, imaging was performed in both the SKOV-3 and BT474 xenograft models. In one study, 5 athymic mice bearing SKOV-3 xenografts were administered with 2.6–3.8 MBq (1.0–1.5 μg) [^{18}F]TFPFN-5F7; two mice received trastuzumab (4.4 mg in 200 μL; ~200 mg/kg) intravenously 24 h prior to injecting the tracer. The tracer-only mice were imaged at 1 h and 2 h while mice pre-treated with trastuzumab were imaged at 1 h. In a second study, 6 mice bearing BT474 subcutaneous xenografts were imaged after administration of 1.8–6.1 MBq (1.3–4.3 μg) of [^{18}F]TFPFN-5F7 at 1 h (n=4) and 2 h (n=6). In all imaging studies, mice were anesthetized using 2–3% isoflurane in oxygen and placed prone in the scanner gantry for a 5-min static PET acquisition followed by a 5 min CT scan. List mode PET data were histogram-processed, and the images reconstructed using the standard OSEM3D/MAP

Author Manuscript Author Manuscript Author Manuscript Author Manuscript

algorithm—2 OSEM3D iterations, and 18 MAP iterations—with a cutoff (Nyquist) of 0.5. Images were corrected for attenuation (CT-based) and radioactive decay. Image analysis was performed using the Inveon Research Workplace software (Siemens).

RESULTS

Chemistry and Radiochemistry.

DCC-mediated coupling of 6-fluoronicotinic acid with 2,3,5,6-tetrafluorophenol was used for the synthesis of **1** (Scheme 1), which was obtained in 41% isolated yield. Its NMR and mass spectral data were consistent with the structure.

The decay-corrected radiochemical yield for the synthesis of [^{18}F]**1** including HPLC purification was 23.4 ± 11.2 % (n = 15) and, on average, ~600 MBq of [^{18}F]**1** could be obtained starting with 3.7 GBq of [^{18}F]fluoride in about 1 h. The prosthetic agent [^{18}F]**1** was conjugated to 2Rs15d and 5F7 sdAbs in decay-corrected radiochemical yields of 24.2 ± 10.4% (n = 8) and 17.1 ± 2.6 % (n = 4), respectively, in 35 min (Scheme 2). The overall decay-corrected radiochemical yield for the synthesis of [^{18}F]TFPFN-2Rs15d and [^{18}F]TFPFN-5F7 was 5.7 ± 3.6% and 4.0 ± 2.0%, respectively. About 116 and 81 MBq of [^{18}F]TFPFN-2Rs15d and [^{18}F]TFPFN-5F7 could be prepared starting from 3.7 GBq of [^{18}F]fluoride in 95 min.

Quality control of [^{18}F]TFPFN-sdAb.

The specific activity was in the range of 0.2 – 0.9 MBq/μg and 0.7 – 2.5 MBq/μg for [^{18}F]TFPFN-2Rs15d and [^{18}F]TFPFN-5F7, respectively. SDS-PAGE/phosphor imaging of [^{18}F]TFPFN-2Rs15d indicated a single radioactive band, which corresponded to the molecular weight of 2Rs15d sdAb (Figure 1A). Size-exclusion HPLC (Figure 1 B) also indicated one major peak corresponding to a molecular weight of ~13 kDa. In some cases, protein-associated activity for [^{18}F]TFPFN-2Rs15d preparations was determined by TCA precipitability and was 98.4 ± 0.1%. The immunoreactive fraction (IRF), determined by Lindmo assay, for [^{18}F]TFPFN-2Rs15d was 62.5 ± 7.8% (Figure 1C). A saturation binding assay using BT474M1 cells gave a K_d value of 4.7 ± 1.2 nM (Figure 1D); with SKOV-3 cells, a K_d value of 10.3 ± 1.1 nM was obtained. The radiochemical purity of [^{18}F]TFPFN-5F7 was slightly lower than that seen for [^{18}F]TFPFN-2Rs15d; aggregates and small molecules accounting for a total of ~5% was seen in SDS PAGE/phosphor imaging; IRF of 57.3% was obtained. K_d values of 2.7 ± 0.6 nM and 4.3 ± 0.5 nM, respectively were obtained with SKOV-3 and BT474M1 cells, respectively.

Paired-label Internalization Assays with [^{18}F]TFPFN-sdAb conjugates.

With the [^{18}F]TFPFN-2Rs15d and [^{125}I]SGMIB-2Rs15d tandem, the assay was performed using both SKOV-3 and BT474M1 cell lines. The percentages of activity initially bound to cells, remaining bound to the cells and that present in the intracellular compartment as a function of incubation time are presented in Figure 2. About 11–13% of the input activity was taken up by SKOV-3 cells after a 1 h incubation at 4°C for both 2Rs15d radioconjugates; nonspecific uptake was about 3% and 10% of total uptake for [^{18}F]TFPFN-2Rs15d and [^{125}I]SGMIB-2Rs15d, respectively. The percentage of initially

Author Manuscript Author Manuscript Author Manuscript Author Manuscript

bound activity that was intracellularly trapped was about 19–21% for [^{18}F]TFPFN-2Rs15d compared with 19–25% for [^{125}I]SGMIB-2Rs15d (Figure 2A). The difference in the internalized activity between the two tracers was significant by paired *t*-test ($P < 0.05$) only at 4 h. The percentage of initially bound activity that remained cell-associated (surface-bound plus internalized) was similar for both tracers at the 3 time points (Figure 2B); however, the difference at 4 h was statistically significant ($P = 0.02$). The data obtained from the assay using BT474M1 cells are shown in Figure 2C and 2D and exhibited similar behavior to that observed with SKOV-3 cells.

In the case of 5F7, paired-label assays were performed using BT474M1 cells only; internalization assay was conducted in a single-label format with [^{18}F]TFPFN-5F7 on SKOV-3 cells. In the assay using [^{18}F]TFPFN-5F7 and *iso*-[^{125}I]SGMIB-5F7 pair, 8–9% of input activity for [^{18}F]TFPFN-5F7 bound to BT474M1 cells compared with 13–15% for *iso*-[^{125}I]SGMIB-5F7; nonspecific uptake was about 13% and 9%, respectively, of initial total cell-bound activity. The percentage of initially bound activity that was intracellularly trapped was similar ($P > 0.05$) for both tracers — 37–57% for [^{18}F]TFPFN-5F7 and 35–53% for *iso*-[^{125}I]SGMIB-5F7 (Figure 3A). The total cell-bound activity (surface-bound plus internalized) was also similar for both tracers at the three time points (Figure 3B); however, the difference at 1 h and 4 h was statistically significant ($P = 0.006$ and 0.001).

In Vivo Studies with [^{18}F]TFPFN-2Rs15d

Paired-label biodistribution of [^{18}F]TFPFN-2Rs15d and [^{125}I]SGMIB-2Rs15d.— Results for the tissue distribution of [^{18}F]TFPFN-2Rs15d and [^{125}I]SGMIB-2Rs15d in athymic mice with subcutaneous HER2-expressing SKOV-3 xenografts are summarized in Table 1. Uptake in tumor was similar at 1 h and 2 h for both tracers; however, it was slightly higher for [^{125}I]SGMIB-2Rs15d at 3 h (3.6 ± 1.7 %ID/g versus 2.9 ± 1.4 %ID/g; $P < 0.05$). On the other hand, renal levels of [^{18}F]TFPFN-2Rs15d was substantially (2.5-, 4.6-, and 8.7-fold; $P < 0.05$) lower than that observed for [^{125}I]SGMIB-2Rs15d. With regard to other normal tissues, retention of activity was quite low and declined with time. At 1 h, uptake of ^{18}F was higher than that seen for ^{125}I in liver, spleen, lungs, and heart but the opposite was seen at 2 h and 3 h. Uptake in blood was 3.7-, 1.8-, and 1.2-fold higher for ^{18}F but the difference was statistically significant ($P < 0.05$) only at 1 h. A similar trend was seen in muscle with the uptake of ^{18}F 1.6-fold higher ($P < 0.05$) at 1 h but the difference between the uptake of the two tracers was not statistically significant at 2 h and 3 h. While bone uptake was higher for ^{18}F compared with ^{125}I at all three time points, absolute levels were low suggesting defluorination of [^{18}F]TFPFN-2Rs15d was minimal. Tumor-to-normal tissue ratios for the two tracers are presented in Figure 4. The most notable difference was observed in kidney, where tumor-to-normal tissue ratios for [^{18}F]TFPFN-2Rs15d were about 2- to 8-fold higher than those for [^{125}I]SGMIB-2Rs15d. Tumor-to-normal tissue ratios for both tracers were generally similar in blood, lungs, liver, spleen and muscle, and were >5:1 in all tissues except kidneys by 2 h post injection.

MicroPET/CT imaging with [^{18}F]TFPFN-2Rs15d.—Maximum intensity projection images obtained at 1 h, 2 h, and 3 h after injection of [^{18}F]TFPFN-2Rs15d in one of the athymic mice bearing SKOV-3 xenografts are shown in Figure 5. Concordant with the

Author Manuscript Author Manuscript Author Manuscript Author Manuscript

biodistribution data, kidneys and bladder were the only organs other than tumor with prominent activity. By 3 h, most of the activity accumulated in the kidneys has been eliminated, resulting in a high contrast image of the tumor. The SUV-Max (%ID/g) for tumor in this mouse calculated from the imaging data was 1.2 (4.6 %ID/g), 1.2 (4.5 %ID/g) and 1.0 (3.7 %ID/g) at 1 h, 2 h, and 3 h, respectively. Tumor-to-muscle ratios were 20.0 and 60 at 1 h and 2 h; due to negligible activity in muscle, this ratio could not be obtained at 3 h.

In Vivo Studies with [^{18}F]TFPFN-5F7

Paired-label biodistribution of [^{18}F]TFPFN-5F7 and iso-[^{125}I]SGMIB-5F7.—The %ID/g uptake values obtained in athymic mice for tumor and normal tissues 2 h after administration of *iso*-[^{125}I]SGMIB-5F7 and [^{18}F]TFPFN-5F7 in athymic mice bearing BT474 xenografts are shown in Figure 6. With both radiolabeled sdAb conjugates, tumor had the highest uptake and, except for kidneys, uptake in other tissues was considerably lower. Tumor uptake of [^{18}F]TFPFN-5F7 was only about 72% of that seen for *iso*-[^{125}I]SGMIB-5F7 (10.9 ± 2.6 %ID/g versus 15.2 ± 3.5 %ID/g; P = 0.004). On the other hand, kidney uptake of [^{18}F]TFPFN-5F7 was less than a third of that for *iso*-[^{125}I]SGMIB-5F7 (2.4 ± 0.3 %ID/g versus 8.4 ± 3.1 %ID/g; P = 0.01). Uptake in lungs and bone for [^{18}F]TFPFN-5F7 was significantly higher than that observed for *iso*-[^{125}I]SGMIB-5F7. The tumor-to-kidney ratio was about 2-fold higher for [^{18}F]TFPFN-5F7, on the other hand, tumor-to-tissue ratios for lungs, bone and blood were higher for [^{125}I]SGMIB-5F7.

MicroPET/CT imaging with [^{18}F]TFPFN-5F7.—Figure 7A shows the maximum intensity projection images obtained in one of the three athymic mice bearing SKOV-3 xenograft at 1 h and 2 h after administration of [^{18}F]TFNFP-5F7. While there was some uptake in kidneys, liver, and lungs at 1 h, most of the activity was cleared by 2 h and only tumor and bladder were clearly visible. Tumor uptake values (SUV Max) calculated from these imaging data were 1.5 (6.8 %ID/g) and 1.5 (6.6 ± 1.7 %ID/g) at 1 h and 2 h, respectively. The tumor-to-muscle tissue ratio was 30 at both time points. Figure 7B is an image obtained at 1 h in a mouse with SKOV-3 xenograft that had received trastuzumab 24 h before administering [^{18}F]TFNFP-5F7. In this case, uptake in tumor was much lower with a SUV-Max of 0.7 (2.3% ID/g), demonstrating that uptake in tumor was HER2-specific.

Maximum intensity projection images obtained after administration of [^{18}F]TFPFN-5F7 in a representative athymic mouse with a subcutaneous BT474 xenograft are shown in Figure 8. The tumor was well delineated even at 1 h with some activity in kidneys and bladder. By 2 h, the only organ other than tumor with prominent activity was the bladder. The tumor SUV-Max values obtained from this imaging data were 3.6 (13.7 %ID/g) and 3.5 (13.4 %ID/g) at 1 h and 2 h, respectively and the tumor-to-muscle ratios were 40 and 70.

DISCUSSION

Methods to assess HER2 levels in breast carcinoma patients by PET imaging are evolving and sdAbs have shown promise as a targeting vector for this purpose. In common with other proteins with molecular weights less than ~60 kDa, a significant problem associated with radiolabeled sdAb is their high uptake in kidneys. Our earlier work has shown than tumor

Author Manuscript Author Manuscript Author Manuscript Author Manuscript

uptake of ^{18}F-labeled sdAbs that target internalizing receptors such as HER2 can be augmented by using residualizing prosthetic agents; however, this strategy resulted in very high uptake in the kidneys.[24, 25] On the other hand, labeling the HER2-reactive sdAb 5F7 using the standard ^{18}F-labeling prosthetic agent [^{18}F]SFB resulted in lower tumor uptake but substantially lower kidney uptake compared with 5F7 labeled using a residualizing prosthetic agent.[24] Building on earlier studies with heavier halogens, in this work, we explored the potential of labeling sdAbs using an agent containing a pyridine ring in lieu of the benzene ring in [^{18}F]SFB, with the objective of attempting to achieve tumor residualizing effect over a time course relevant to the half-life of ^{18}F without excessive kidney uptake.

Our first choice for the pyridine-based prosthetic agent was [^{18}F]SFN, derived by substituting a pyridine ring for the benzene ring in [^{18}F]SFB. Although details are not included herein, we initially attempted synthesis of both unlabeled and [^{18}F]SFN, the latter via a one pot, three-step method similar to that reported for [^{18}F]SFB,[47] from the quaternary ammonium salt precursor, 5-(methoxycarbonyl)-*N,N,N*-trimethylpyridin-2-aminium trifluoromethanesulfonate. In a few attempts, conjugation of 2Rs15d with [^{18}F]SFN resulted in meager yields (5% at best), presumably due to hydrolytic instability of [^{18}F]SFN at pH 8.5 (see below).

Having had no success with [^{18}F]SFN, we decided to employ the 2,3,5,6-tetrafluorophenyl ester [^{18}F]**1**, first reported by Olberg et al.[30] It is known that the hydrolytic stability of 2,3,5,6-tetrafluorophenyl esters is better than that of the corresponding NHS ester at a pH of ~8 (half-life for hydrolysis about twice longer).[48, 49] Furthermore, 2,3,5,6-tetrafluorophenyl esters are known to undergo facile aminolysis.[50, 51] Although the precursor **2** was synthesized following the procedure reported by Olberg et al.,[30] we used a different method from that reported by these investigators for the synthesis of the unlabeled **1** standard. They adapted the ^{18}F-labeling conditions for the synthesis of unlabeled **1** by reacting the quaternary salt precursor with potassium fluoride in the presence of Kryptofix222. We synthesized **1** by the simple dicyclohexylcarbodiimide-mediated esterification of 6-fluoronicotinic acid with 2,3,5,6-tetrafluorophenol.

For the synthesis of [^{18}F]**1**, we adapted a recently reported simple, on-cartridge method.[31, 32] It is a very convenient method because the routinely employed azeotropic drying of water from aqueous solutions of [^{18}F]fluoride can be bypassed, with the labeling taking place on the cartridge at room temperature even as the cartridge is eluted with the solution of the quaternary salt precursor. However, we found that use of the prescribed[31] 1 mL of precursor solution in one portion did not elute all of the ^{18}F-activity from the Chromafix® 30-PS-HCO_3 cartridge; ~50% of the activity remained in the cartridge. On the other hand, ~75% of the activity could be recovered from the cartridge by dividing the precursor solution into two equal portions and eluting the cartridge twice. The overall yield we obtained for the synthesis of [^{18}F]**1** was lower than that reported by Basuli et al.[31] mainly because we included an HPLC purification step to avoid complications related to the presence of a substantial amount of the byproduct 2,3,5,6-tetrafluorophenyl 6-(2,3,5,6-tetrafluorophenoxy)nicotinate.[30, 31] Because this byproduct contains an active ester, it can compete with [^{18}F]**1** for reaction with the amino groups of proteins such as sdAbs, lowering

Author Manuscript Author Manuscript Author Manuscript Author Manuscript

conjugation yields. Basuli et al.,[32] used [^{18}F]**1** without separating it from the byproduct for conjugation to albumin; however, 20 mg protein was used. Because injected doses with labeled sdAbs have only been 1 mg or less even for clinical studies,[13] and the potential for compromising sdAb biological properties due to byproduct conjugation, we considered removal of the byproduct from [^{18}F]**1** to be essential. Using the HPLC conditions described herein, it was possible to separate the byproduct from the desired labeled product. Volatility of [^{18}F]**1** was a significant problem that has not been reported previously. Although extreme care was taken to minimize volatilization loss during the two evaporation steps in the synthesis of [^{18}F]**1**, substantial and variable amounts of activity loss did occur. There was 15%−45% loss during the evaporation of the eluate from the MCX cartridge and about 5% loss during the evaporation of the HPLC fractions. We note that it has been reported that 2,3,5,6-tetrafluorophenyl 2-[^{18}F]fluoropropionate is volatile but the corresponding 4-nitrophenyl ester is not.[52] In future studies, we may explore the utility of the 4-nitrophenyl ester of 6-fluoronicotinic acid or other approaches to mitigate this issue. Despite these problems, it was possible to synthesize [^{18}F]**1** in reasonable yields and in a shorter total synthesis time than needed for the synthesis of [^{18}F]RL-I;[37] indeed, about 3-fold higher yield was obtained in about three quarters of the time. On the other hand, yield for the synthesis of [^{18}F]**1** was lower than that obtained for another residualizing prosthetic agent [^{18}F]RL-II,[36] although the duration of synthesis was slightly shorter for [^{18}F]**1**. While cassette-based and continuous flow automated syntheses have been developed for the benchmark prosthetic agent for biomolecule labeling, [^{18}F]SFB,[53–56] the manual synthesis of [^{18}F]**1** is more streamlined than that utilized for [^{18}F]SFB; it is highly likely that automated synthetic methods will be developed for [^{18}F]TFPFN in the near future.

The average conjugation yields obtained for labeling the two sdAbs with [^{18}F]**1** were about 15–25%, which are lower than those observed with *N*-hydroxysuccinimidyl ester-containing radiolabeled prosthetic agents.[23, 37, 57] Potential reasons for the lower coupling yields with [^{18}F]**1** include rapid hydrolysis of the reagent and/or the presence of competing active ester impurities. With regard to the first possibility, as noted earlier, TFP esters are more stable than NHS esters and consistent with this, our preliminary studies indicated that [^{18}F]SFN was hydrolytically unstable. In contrast, similar instability of its benzylic analogue [^{18}F]SFB has not been observed suggesting that nicotinates such as SFN and TFPFN are more susceptible to hydrolysis than analogous benzoates. This explanation is further supported by the fact that protein conjugation yields for the analogous radioiodinated benzoate ester, SIB, are significantly higher than those for the nicotinate analogue, SIPC.[58] With regard to the second possibility, TFPFN (t_R = 9.1 min) and the byproduct 2,3,5,6-tetrafluorophenyl 6-(2,3,5,6-tetrafluorophenoxy)nicotinate (t_R = 6.5 min) are separable by HPLC; however, because the byproduct is formed in significant amounts, it could potentially bleed into [^{18}F]**1** fractions. Indeed, in quality control HPLC of [^{18}F]**1**, we occasionally have seen the presence of the byproduct. In addition, the presence of carrier, formed either via the [^{19}F]fluoride present in [^{18}F]fluoride or through exchange with the fluorine in the substrate, has also been seen occasionally.

The affinity and immunoreactivity of both anti-HER2 sdAbs were comparable to those obtained when 2Rs15d and 5F7 were conjugated to other prosthetic agents labeled with

Author Manuscript Author Manuscript Author Manuscript Author Manuscript

^{18}F[24, 25, 36] as well as other radionuclides.[12, 23, 33] Surface plasmon resonance measurements indicate that the binding affinity of unmodified 2Rs15d and 5F7 are 3.9 nM[38] and 0.5 nM,[40] respectively. The binding affinity of the [^{18}F]TFPFN-sdAb conjugates determined by saturation binding assays on HER2-positive cancer cells were somewhat lower, particularly in the case of [^{18}F]TFPFN-5F7. This may reflect the fact that none of the lysines in 2Rs15d are in the HER2 binding region[12] while one of the lysines in 5F7 is in its CDR2 region.[40] Nonetheless, the binding of [^{18}F]TFPFN-5F7 on both SKOV-3 and BT474M1 cell lines was better than that obtained for [^{18}F]TFPFN-2Rs15d, reflecting the higher affinity of unlabeled 5F7 for the HER2 molecule.

The percentage of initially bound activity from [^{18}F]TFPFN-2Rs15d that was present in the intracellular compartment about 20% on both the SKOV-3 and BT474M1 cell lines, values that were quite similar to those obtained for co-incubated [^{125}I]SGMIB. Thus, with a slowly internalizing anti-HER2 sdAb like 2Rs15d, the fluoronicotinoyl prosthetic moiety provides adequate cellular trapping over a time course relevant to the half-life of ^{18}F. Consistent with the results of previous studies with radiolabeled versions of the two anti-HER2 sdAbs,[23–25] internalized activity for [^{18}F]TFPFN-5F7 was significantly higher than that observed for [^{18}F]TFPFN-2Rs15d with similar differences observed for the corresponding radioiodinated sdAb conjugates. The two sdAbs bind to different epitopes on the HER2 molecule,[12] which might account for dissimilar rates of internalization and subsequent intracellular catabolism. However, with a more rapidly internalizing sdAb like 5F7, the residualizing capacity of the radiolabeled prosthetic agent could be more important. In a previous study, we observed similar behavior in intracellular trapping when the residualizing agents [^{18}F]RL-I and [^{125}I]SGMIB were used to label 5F7.[24] In marked contrast, when 5F7 labeling was done with [^{18}F]SFB, after a 4-h incubation, intracellular activity had decreased to less than half that seen with [^{125}I]SGMIB.[24] Thus, it was encouraging to note that intracellular trapping and total cell-associated activity for [18F]TFPFN-5F7 was quite similar to that observed for co-incubated radioiodinated, guanidine 5F7 conjugate over the 4-h study period.

As seen in SKOV-3 cells in vitro, the tumor uptake of [^{18}F]TFPFN-2Rs15d in subcutaneous SKOV-3 xenografts was similar to that seen for co-injected [^{125}I]SGMIB-2Rs15d over the 3-h experimental period. Similar results were observed in a previous study in this xenograft model, in which the tumor uptake of 2Rs15d labeled using the [^{18}F]RL-II residualizing prosthetic agent, was similar to that of co-administered [^{125}I]SGMIB-2Rs15d.[36] While the tumor uptake seen for [^{18}F]TFPFN-2Rs15d was somewhat lower than that seen for [^{18}F]RL-II-2Rs15d, the kidney uptake was about 10-fold lower. Although, as noted above, tumor uptake of [^{18}F]TFPFN-2Rs15d at 1 h was virtually identical to that observed using the prototypical residualizing agent SGMIB, it was somewhat lower than that reported for a single label study with [^{18}F]SFB-2Rs15d (3.73 ± 1.14 %ID/g versus 5.94 ± 1.17 %ID/g).[57] This likely reflects differences in the characteristics of human tumor xenografts that are known to occur among groups of experimental animals, which is the reason we prefer to perform biodistribution experiments with a reference compound when possible. Reducing kidney uptake while maintaining adequate tumor levels is an important objective for developing sdAb-based imaging agents. Tumor-to-kidney ratios for [^{18}F]TFPFN-2Rs15d at 1 h were virtually identical to those reported by Xavier et al.;[57] however, by 3 h after injection, tumor to kidney ratios were almost 3-fold higher with the new reagent

Author Manuscript Author Manuscript Author Manuscript Author Manuscript

([^{18}F]TFPFN, 2.9:1; [^{18}F]SFB, 1.0:1). Consistent with these necropsy biodistribution experiments, high contrast PET images could be obtained after administration of [^{18}F]TFPFN-2Rs15d in the SKOV-3 xenograft model. While there was some uptake in liver and lungs, and high activity levels in kidneys and bladder at 1 h, normal tissue clearance was rapid such that by 3 h, the only organ other than tumor that was visualized was the bladder.

Because of the more extensive internalization of anti-HER2 5F7 sdAb, achieving good residualization after receptor binding with it could play a greater role than in the case of the modestly internalizing 2Rs15d construct. From the microPET imaging studies, uptake of [^{18}F]TFPFN-5F7 in SKOV-3 xenografts remained constant between 1-h and 2-h time points, suggesting good residualization had been achieved as observed with [^{18}F]TFPFN-2Rs15d. However, the magnitude of tumor uptake was about 50% higher for [^{18}F]TFPFN-5F7 (6.6 and 6.8% ID/g at 1 and 2 h) compared with [^{18}F]TFPFN-2Rs15d (4.6 and 4.5% ID/g at 1 and 2 h), suggesting a potential advantage of combining a more extensively internalized anti-HER2 sdAb with a residualizing labeling method. Moreover, the uptake of [^{18}F]TFPFN-5F7 in tumor was shown to be mediated by HER2 binding because pretreatment of mice with trastuzumab, which competes with 5F7 for its HER2 binding site, significantly decreased tumor uptake.

To the best of our knowledge, no studies have been reported describing the in vivo behavior of other radiolabeled 5F7 conjugates in the SKOV-3 xenograft model to make comparisons. On the other hand, the biodistribution of 5F7 after labeling with ^{18}F, $^{125/131}$I, and ^{211}At in xenografts derived from the BT474 human breast carcinoma cell line have been reported, [14, 23, 24, 40] providing useful benchmarks for comparison. We note that one of these studies demonstrated the superiority of *iso*-SGMIB compared with the original SGMIB isomer for labeling 5F7,[14] which is the reason *iso*-[^{125}I]SGMIB-5F7 was used as comparator for [^{18}F]TFPFN-5F7. In the necropsy biodistribution experiment, uptake of [^{18}F]TFPFN-5F7 in BT474 xenografts 2 h after injection (10.9 ± 2.6 %ID/g) was only about 70% of that observed for co-injected *iso*-[^{125}I]SGMIB-5F7. In comparison, tumor uptake of for [^{18}F]RL-I-5F7 was essentially the same as that for co-administered [^{125}I]SGMIB-5F7 in the BT474M1 xenograft model.[24] Although differences in residualizing capacity of the two ^{18}F prosthetic agents could play a role, the higher xenograft uptake of *iso*-[^{125}I]SGMIB-5F7 compared with [^{125}I]SGMIB-5F7 is probably a contributing factor. As was observed in the SKOV-3 model, renal uptake of [^{18}F]TFPFN-5F7 was considerably lower than its radioiodinated counterpart in the BT474 model as well. Furthermore, it was somewhat lower than that seen with [^{18}F]SFB-5F7 and more than 50-fold lower compared with that observed for [^{18}F]RL-I-5F7.[24] Consistent with the results from the necropsy experiment, microPET imaging showed excellent visualization of these subcutaneous BT474 xenografts with only tumor and bladder being visible at 2 h. Quantification of tumor uptake from imaging studies indicated a high degree of tumor uptake (greater than 13% ID/g at 1 h and 2 h) with tumor:muscle ratios greater than 50:1 seen 2 h after injection. The higher tumor uptake observed in BT474 vs SKOV-3 xenografts is consistent with previous studies and likely reflects differences in HER2 expression levels in these models.[12]

Author Manuscript Author Manuscript Author Manuscript Author Manuscript

CONCLUSION

Herein we have labeled two anti-HER2 single domain antibody fragments with ^{18}F using the fluoropyridine-containing prosthetic agent [^{18}F]TFPFN. The HER2-reactive sdAbs thus labeled retained affinity and immunoreactivity to the target antigen. There was a substantial advantage for this labeling method with respect to kidney uptake compared with previously developed residualizing prosthetic agents for ^{18}F labeling, RL-I and RL-II. Higher tumor uptake levels were obtained when [^{18}F]TFPFN was used in tandem of the sdAb undergoing greater internalization after receptor binding. In the case of the more modestly internalizing sdAb 2Rs15d, tumor uptake was comparable to that reported for [^{18}F]SFB-2Rs15d; however, there was some advantage with respect to clearance of activity from the kidneys. Given that the manual synthesis of [^{18}F]TFPFN is more facile than that of [^{18}F]SFB and that it has yet to be fully optimized, our results suggest that [^{18}F]TFPFN warrants further investigation as a method for labeling sdAbs and other low molecular weight proteins.

ACKNOWLEDGEMENTS

This work was generously funded by Grants CA188177 and CA42324 from the National Institutes of Health. The excellent technical assistance of Elzbieta Krol (in vitro studies) and Xiao-Guang Zhao (in vivo studies) is greatly appreciated. We also thank Thomas Hawk, and Simone Degan for their excellent support with micro-PET/CT imaging studies.

ABBREVIATIONS USED (UNCOMMON)

APCI	atmospheric pressure chemical ionization
ASAP	atmospheric solids analysis probe
HSA	human serum albumin
***iso*-SGMIB**	*N*-succinimidyl 3-guanidinomethyl-5-iodobenzoate
NHS	*N*-hydroxysuccinimidyl
PET/CT	positron emission tomography/computed tomography
sdAb	single domain antibody fragment
SFB	*N*-succinimidyl 4-fluorobenzoate
SFBTMGMB (RL-I)	*N*-succinimidyl 3-((4-(4-fluorobutyl)-1*H*-1,2,3-triazol-1-yl)methyl)-5-(guanidinomethyl)benzoate
SGMIB	*N*-succinimidyl 4-guanidinomethyl-3-iodobenzoate
SIPC	*N*-succinimidyl 5-iodo-3-pyridinecarboxylate
TFP	2,3,5,6-tetrafluorophenyl
TFPFN	2,3,5,6-tetrafluorophenyl 6-fluoronicotinate.

Author Manuscript Author Manuscript Author Manuscript Author Manuscript

REFERENCES

1. Hou Y; Nitta H; Wei L; Banks PM; Portier B; Parwani AV; Li Z HER2 intratumoral heterogeneity is independently associated with incomplete response to anti-HER2 neoadjuvant chemotherapy in HER2-positive breast carcinoma. Breast. Cancer Res. Treat 2017, 166(2), 447–57. [PubMed: 28799059]
2. Duffy MJ; Harbeck N; Nap M; Molina R; Nicolini A; Senkus E; Cardoso F Clinical use of biomarkers in breast cancer: Updated guidelines from the European Group on Tumor Markers (EGTM). Eur. J. Cancer 2017, 75, 284–98. [PubMed: 28259011]
3. Olafsen T; Sirk SJ; Olma S; Shen CK; Wu AM ImmunoPET using engineered antibody fragments: fluorine-18 labeled diabodies for same-day imaging. Tumour Biol 2012, 33 (3), 669–77. [PubMed: 22392499]
4. Ueda M; Hisada H; Temma T; Shimizu Y; Kimura H; Ono M; Nakamoto Y; Togashi K; Saji H Gallium-68-labeled anti-HER2 single-chain Fv fragment: development and in vivo monitoring of HER2 expression. Mol. Imaging Biol 2015, 17 (1), 102–10. [PubMed: 25049073]
5. Ulaner GA; Lyashchenko SK; Riedl C; Ruan S; Zanzonico PB; Lake D; Jhaveri K; Zeglis B; Lewis JS; O'Donoghue JA First-in-human HER2-targeted imaging using ^{89}Zr-pertuzumab PET/CT: Dosimetry and clinical application in patients with breast cancer. J. Nucl. Med 2018, 59 (6), 900–6. [PubMed: 29146695]
6. Tolmachev V; Yim CB; Rajander J; Perols A; Karlstrom AE; Haaparanta-Solin M; Gronroos TJ; Solin O; Orlova A Comparative evaluation of anti-HER2 affibody molecules labeled with 64Cu using NOTA and NODAGA. Contrast Media Mol. Imaging 2017, DOI: 10.1155/2017/8565802.
7. Gonzalez-Sapienza G; Rossotti MA; Tabares-da Rosa S Single-domain antibodies as versatile affinity reagents for analytical and diagnostic applications. Front. Immunol 2017, 8, DOI: 10.3389/fimmu.2017.00977.
8. Schumacher D; Helma J; Schneider AFL; Leonhardt H; Hackenberger C Chemical functionalization strategies and intracellular applications of nanobodies. Angew. Chem. Int. Ed. Engl 2017, 57 (9), 2314–33.
9. Leow CH; Fischer K; Leow CY; Cheng Q; Chuah C; McCarthy J Single domain antibodies as new biomarker detectors. Diagnostics (Basel) 2017, 7 (52), 10.3390/diagnostics7040052.
10. Van Audenhove I; Gettemans J Nanobodies as versatile tools to understand, diagnose, visualize and treat cancer. EBioMedicine 2016, 8, 40–8. [PubMed: 27428417]
11. Steeland S; Vandenbroucke RE; Libert C Nanobodies as therapeutics: big opportunities for small antibodies. Drug Discov. Today 2016, 21, (7), 1076–113. [PubMed: 27080147]
12. D'Huyvetter M; De Vos J; Xavier C; Pruszynski M; Sterckx YGJ; Massa S; Raes G; Caveliers V; Zalutsky M; Lahoutte T; Devoogdt N ^{131}I-labeled anti-HER2 camelid sdAb as a theranostic tool in cancer treatment. Clin. Cancer Res 2017, 23 (21), 6616–28. [PubMed: 28751451]
13. Keyaerts M; Xavier C; Heemskerk J; Devoogdt N; Everaert H; Ackaert C; Vanhoeij M; Duhoux FP; Gevaert T; Simon P; Schallier D; Fontaine C; Vaneycken I; Vanhove C; De Greve J; Lamote J; Caveliers V; Lahoutte T Phase I study of ^{68}Ga-HER2-Nanobody for PET/CT assessment of HER2 expression in breast carcinoma. J. Nucl. Med 2016, 57 (1), 27–33 [PubMed: 26449837]
14. Choi J; Vaidyanathan G; Koumarianou E; Kang CM; Zalutsky MR Astatine-211 labeled anti-HER2 5F7 single domain antibody fragment conjugates: radiolabeling and preliminary evaluation. Nucl. Med. Biol 2017, 56, 10–20. [PubMed: 29031230]
15. Krasniqi A; D'Huyvetter M; Devoogdt N; Frejd FY; Sorensen J; Orlova A; Keyaerts M; Tolmachev V Same-day imaging using small proteins: Clinical experience and translational prospects in oncology. J. Nucl. Med 2018, 59 (6), 885–91. [PubMed: 29545374]
16. Sanchez-Crespo A Comparison of Gallium-68 and Fluorine-18 imaging characteristics in positron emission tomography. Appl. Radiat. Isot 2013, 76, 55–62. [PubMed: 23063597]
17. Coenen HH; Elsinga PH; Iwata R; Kilbourn MR; Pillai MR; Rajan MG; Wagner HN Jr.; Zaknun JJ Fluorine-18 radiopharmaceuticals beyond [^{18}F]FDG for use in oncology and neurosciences. Nucl. Med. Biol 2010, 37 (7), 727–40. [PubMed: 20870148]

Author Manuscript Author Manuscript Author Manuscript Author Manuscript

18. Clark J; O'Hagan D Strategies for radiolabelling antibody, antibody fragments and affibodies with fluorine-18 as tracers for positron emission tomography (PET). J. Fluorine Chem 2017, 203, 31–46.
19. Li XG; Haaparanta M; Solin O Oxime formation for fluorine-18 labeling of peptides and proteins for positron emission tomography (PET) imaging: A review. J Fluorine Chem 2012, 143, 49–56.
20. Richter S; Wuest F ^{18}F-Labeled peptides: The future is bright. Molecules 2014, 19 (12), 20536–56. [PubMed: 25493636]
21. Laverman P; McBride WJ; Sharkey RM; Goldenberg DM; Boerman OC Al^{18}F labeling of peptides and proteins. J. Labelled Comp. Radiopharm 2014, 57 (4), 219–23. [PubMed: 24408125]
22. Vaidyanathan G; Zalutsky MR Labeling proteins with fluorine-18 using N-succinimidyl 4-[^{18}F]fluorobenzoate. Int. J. Rad. Appl. Instrum. B 1992, 19 (3), 275–81. [PubMed: 1629016]
23. Pruszynski M; Koumarianou E; Vaidyanathan G; Revets H; Devoogdt N; Lahoutte T; Lyerly HK; Zalutsky MR Improved tumor targeting of anti-HER2 nanobody through N-succinimidyl 4-guanidinomethyl-3-iodobenzoate radiolabeling. J. Nucl. Med 2014, 55 (4), 650–6. [PubMed: 24578241]
24. Vaidyanathan G; McDougald D; Choi J; Koumarianou E; Weitzel D; Osada T; Lyerly HK; Zalutsky MR Preclinical evaluation of ^{18}F-labeled anti-HER2 Nanobody conjugates for imaging HER2 receptor expression by immuno-PET. J. Nucl. Med 2016, 57 (6), 967–73. [PubMed: 26912425]
25. Zhou Z; Vaidyanathan G; McDougald D; Kang CM; Balyasnikova I; Devoogdt N; Ta AN; McNaughton BR; Zalutsky MR Fluorine-18 labeling of the HER2-targeting single-domain antibody 2Rs15d using a residualizing label and preclinical evaluation. Mol. Imaging Biol 2017, 19 (6), 867–877. [PubMed: 28409338]
26. Vaidyanathan G; Zalutsky MR Preparation of N-succinimidyl 3-[*I]iodobenzoate: an agent for the indirect radioiodination of proteins. Nat. Protoc 2006, 1 (2), 707–13. [PubMed: 17406300]
27. Garg S; Garg PK; Zalutsky MR N-succinimidyl 5-(trialkylstannyl)-3-pyridinecarboxylates: a new class of reagents for protein radioiodination. Bioconjug. Chem 1991, 2(1), 50–6. [PubMed: 1878411]
28. Reist CJ; Garg PK; Alston KL; Bigner DD; Zalutsky MR Radioiodination of internalizing monoclonal antibodies using N-succinimidyl 5-iodo-3-pyridinecarboxylate. Cancer Res 1996, 56 (21), 4970–7. [PubMed: 8895752]
29. Siebeneicher H; G. K Formulation of radiopharmaceuticals containing multiple acidic groups 2013,
30. Olberg DE; Arukwe JM; Grace D; Hjelstuen OK; Solbakken M; Kindberg GM; Cuthbertson A One step radiosynthesis of 6-[^{18}F]fluoronicotinic acid 2,3,5,6-tetrafluorophenyl ester ([^{18}F]F-Py-TFP): a new prosthetic group for efficient labeling of biomolecules with fluorine-18. J. Med. Chem 2010, 53 (4), 1732–40. [PubMed: 20088512]
31. Basuli F; Zhang X; Jagoda EM; Choyke PL; Swenson RE Facile room temperature synthesis of fluorine-18 labeled fluoronicotinic acid-2,3,5,6-tetrafluorophenyl ester without azeotropic drying of fluorine-18. Nucl. Med. Biol 2016, 43 (12), 770–2. [PubMed: 27693671]
32. Basuli F; Zhang X; Woodroofe CC; Jagoda EM; Choyke PL; Swenson RE Fast indirect fluorine-18 labeling of protein/peptide using the useful 6-fluoronicotinic acid-2,3,5,6-tetrafluorophenyl prosthetic group: A method comparable to direct fluorination. J. Labelled Comp. Radiopharm 2017, 60 (3), 168–75. [PubMed: 27990672]
33. Pruszynski M; D'Huyvetter M; Bruchertseifer F; Morgenstern A; Lahoutte T Evaluation of an anti-HER2 Nanobody labeled with ^{225}Ac for targeted alpha-particle therapy of cancer. Mol. Pharm 2018, 15 (4), 1457–66. [PubMed: 29502411]
34. Vaidyanathan G; Zalutsky MR Synthesis of N-succinimidyl 4-guanidinomethyl-3-[*I]iodobenzoate: a radioiodination agent for labeling internalizing proteins and peptides. Nat Protoc 2007, 2 (2), 282–6. [PubMed: 17406587]
35. Choi J; Vaidyanathan G; Koumarianou E; McDougald D; Pruszynski M; Osada T; Lahoutte T; Lyerly HK; Zalutsky MR N-succinimidyl guanidinomethyl iodobenzoate protein radiohalogenation agents: influence of isomeric substitution on radiolabeling and target cell residualization. Nucl. Med. Biol 2014, 41 (10), 802–12. [PubMed: 25156548]

Author Manuscript Author Manuscript Author Manuscript Author Manuscript

36. Zhou Z; Chitneni SK; Devoogdt N; Zalutsky MR; Vaidyanathan G Fluorine-18 labeling of an anti-HER2 VHH using a residualizing prosthetic group via a strain-promoted click reaction: Chemistry and preliminary evaluation. Bioorg. Med. Chem 2018, 26 (8), 1939–49. [PubMed: 29534937]
37. Vaidyanathan G; McDougald D; Choi J; Pruszynski M; Koumarianou E; Zhou Z; Zalutsky MR N-succinimidyl 3-((4-(4-[^{18}F]fluorobutyl)-1H-1,2,3-triazol-1-yl)methyl)-5-(guanidinomethyl)ben zoate ([^{18}F]SFBTMGMB): a residualizing label for ^{18}F-labeling of internalizing biomolecules. Org. Biomol. Chem 2016, 14 (4), 1261–71. [PubMed: 26645790]
38. Vaneycken I; Devoogdt N; Van Gassen N; Vincke C; Xavier C; Wernery U; Muyldermans S; Lahoutte T; Caveliers V Preclinical screening of anti-HER2 nanobodies for molecular imaging of breast cancer. FASEB J 2011, 25 (7), 2433–46. [PubMed: 21478264]
39. Xavier C; Vaneycken I; D'Huyvetter M; Heemskerk J; Keyaerts M; Vincke C; Devoogdt N; Muyldermans S; Lahoutte T; Caveliers V Synthesis, preclinical validation, dosimetry, and toxicity of ^{68}Ga-NOTA-anti-HER2 Nanobodies for iPET imaging of HER2 receptor expression in cancer. J. Nucl. Med 2013, 54 (5), 776–84. [PubMed: 23487015]
40. Pruszynski M; Koumarianou E; Vaidyanathan G; Revets H; Devoogdt N; Lahoutte T; Zalutsky MR Targeting breast carcinoma with radioiodinated anti-HER2 Nanobody. Nucl. Med. Biol 2013, 40, (1), 52–9. [PubMed: 23159171]
41. Zhang S; Huang WC; Zhang L; Zhang C; Lowery FJ; Ding Z; Guo H; Wang H; Huang S; Sahin AA; Aldape KD; Steeg PS; Yu D SRC family kinases as novel therapeutic targets to treat breast cancer brain metastases. Cancer Res 2013, 73 (18), 5764–74. [PubMed: 23913825]
42. Marino N; Collins JW; Shen C; Caplen NJ; Merchant AS; Gokmen-Polar Y; Goswami CP; Hoshino T; Qian Y; Sledge GW Jr.; Steeg PS Identification and validation of genes with expression patterns inverse to multiple metastasis suppressor genes in breast cancer cell lines. Clin. Exp. Metastasis 2014, 31 (7), 771–86. [PubMed: 25086928]
43. Cao Y; Marks JD; Huang Q; Rudnick SI; Xiong C; Hittelman WN; Wen X; Marks JW; Cheung LH; Boland K; Li C; Adams GP; Rosenblum MG Single-chain antibody-based immunotoxins targeting Her2/neu: design optimization and impact of affinity on antitumor efficacy and off-target toxicity. Mol. Cancer Ther 2012, 11 (1), 143–53. [PubMed: 22090420]
44. Kim H; Danishmalik SN; Hwang H; Sin JI; Oh J; Cho Y; Lee H; Jeong M; Kim SH; Hong HJ Gene therapy using plasmid DNA-encoded anti-HER2 antibody for cancers that overexpress HER2. Cancer Gene Ther 2016, 23 (10), 341–7. [PubMed: 27632934]
45. Lindmo T; Boven E; Cuttitta F; Fedorko J; Bunn PA Jr. Determination of the immunoreactive fraction of radiolabeled monoclonal antibodies by linear extrapolation to binding at infinite antigen excess. J. Immunol. Methods 1984, 72 (1), 77–89. [PubMed: 6086763]
46. Foulon CF; Reist CJ; Bigner DD; Zalutsky MR Radioiodination via D-amino acid peptide enhances cellular retention and tumor xenograft targeting of an internalizing anti-epidermal growth factor receptor variant III monoclonal antibody. Cancer Res 2000, 60 (16), 4453–60. [PubMed: 10969792]
47. Tang G; Zeng WB; Yu MX; Kabalka G Facile synthesis of N-succinimidyl 4-[^{18}F]fluorobenzoate ([^{18}F]SFB) for protein labeling. J. Labelled Compd. Radiopharm 2008, 51 (1–2), 68–71.
48. Hermanson GT, Bioconjugate Techniques Academic Press: London, UK, 2008.
49. Lockett MR; Phillips MF; Jarecki JL; Peelen D; Smith LM A tetrafluorophenyl activated ester self-assembled monolayer for the immobilization of amine-modified oligonucleotides. Langmuir 2008, 24 (1), 69–75. [PubMed: 18047381]
50. Wilbur DS; Hamlin DK; Srivastava RR; Burns HD Synthesis and radioiodination of N-Boc-p-(tri-n-butylstannyl)-L-phenylalanine tetrafluorophenyl ester: preparation of a radiolabeled phenylalanine derivative for peptide synthesis. Bioconjug. Chem 1993, 4 (6), 574–80 [PubMed: 8305529]
51. Zambianchi M; Di Maria F; Cazzato A; Gigli G; Piacenza M; Della Sala F; Barbarella G Microwave-assisted synthesis of thiophene fluorophores, labeling and multilabeling of monoclonal antibodies, and long lasting staining of fixed cells. J. Am. Chem. Soc 2009, 131 (31), 10892–900. [PubMed: 19618930]
52. Haskali MB; Roselt PD; Karas JA; Noonan W; Wichmann CW; Katsifis A; Hicks RJ; Hutton CA One-step radiosynthesis of 4-nitrophenyl 2-[^{18}F]fluoropropionate ([^{18}F]NFP); improved

Author Manuscript Author Manuscript Author Manuscript Author Manuscript

preparation of radiolabeled peptides for PET imaging. J. Labelled Comp. Radiopharm 2013, 56 (14), 726–30. [PubMed: 24339012]

53. Tang GH; Tang XL; Wang XL A facile automated synthesis of N-succinimidyl 4-[F-18]fluorobenzoate ([F-18]SFB) for F-18-labeled cell-penetrating peptide as PET tracer. J. Labelled Compd. Radiopharm 2010, 53 (7–8), 543–7.
54. Kimura H; Tomatsu K; Saiki H; Arimitsu K; Ono M; Kawashima H; Iwata R; Nakanishi H; Ozeki E; Kuge Y; Saji H Continuous-flow synthesis of N-succinimidyl 4-[^{18}F]fluorobenzoate using a single microfluidic chip. PLoS One 2016, 11 (7), e0159303, DOI:10.1371/journal.pone.0159303.
55. Thonon D; Goblet D; Goukens E; Kaisin G; Paris J; Aerts J; Lignon S; Franci X; Hustinx R; Luxen A Fully automated preparation and conjugation of N-succinimidyl 4-[^{18}F]fluorobenzoate ([^{18}F]SFB) with RGD peptide using a GE FASTlab synthesizer. Mol. Imaging Biol 2011, 13 (6), 1088–95. [PubMed: 21267662]
56. Collins J; Waldmann CM; Drake C; Slavik R; Ha NS; Sergeev M; Lazari M; Shen B; Chin FT; Moore M; Sadeghi S; Phelps ME; Murphy JM; van Dam RM Production of diverse PET probes with limited resources: 24 ^{18}F-labeled compounds prepared with a single radiosynthesizer. Proc. Natl. Acad. Sci. USA 2017, 114 (43), 11309–14. [PubMed: 29073049]
57. Xavier C; Blykers A; Vaneycken I; D'Huyvetter M; Heemskerk J; Lahoutte T; Devoogdt N; Caveliers V ^{18}F-nanobody for PET imaging of HER2 overexpressing tumors. Nucl. Med. Biol 2016, 43 (4), 247–52. [PubMed: 27067045]
58. Garg S; Garg PK; Zhao XG; Friedman HS; Bigner DD; Zalutsky MR Radioiodination of a monoclonal antibody using N-succinimidyl 5-iodo-3-pyridinecarboxylate. Nucl Med Biol 1993, 20 (7), 835–42. [PubMed: 8241995]

Author Manuscript Author Manuscript Author Manuscript Author Manuscript

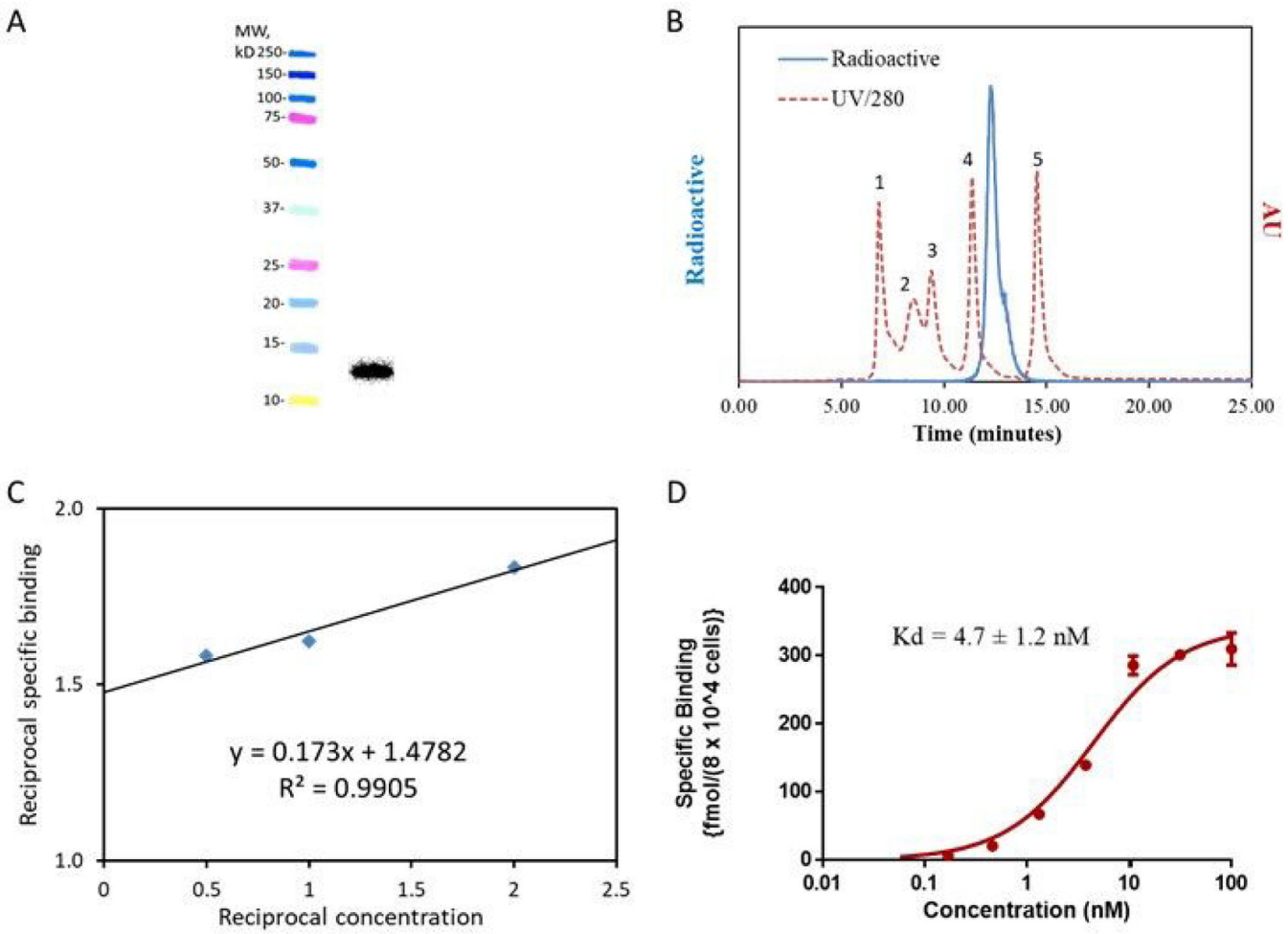

Figure 1.

Evaluation of [^{18}F]TFPFN-2Rs15d conjugate: A) SDS-PAGE; left lane molecular weight markers, right lane [^{18}F]TFPFN-2Rs15d. B) Size-exclusion HPLC; ^{18}F-activity profile in blue; UV HPLC profile of protein molecular weight (red dashed line) — 1 thyroglobulin (670 kDa), 2 γ-globulin (158 kDa), 3 ovalbumin (44 kDa), 4 myoglobin (17 kDa), 5 vitamin B12 (1.4 kDa). C) Double reciprocal plot from the Lindmo immunoreactivity assay. D) Binding affinity determined on BT474M1 cells.

Author Manuscript Author Manuscript Author Manuscript Author Manuscript

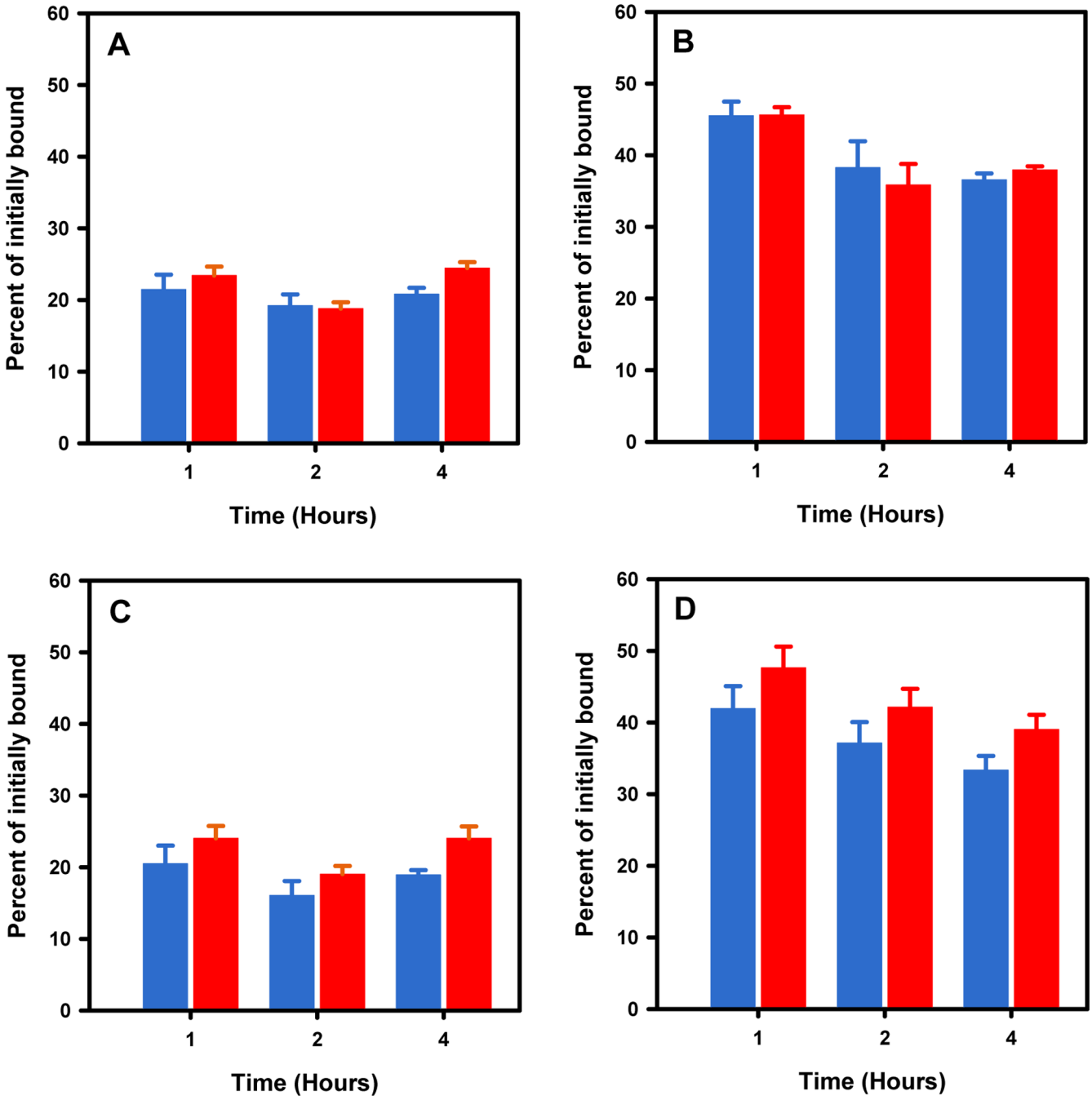

Figure 2.

Paired label internalization of [^{18}F]TFPFN-2Rs15d (blue bars) and [^{125}I]SGMIB-2Rs15d (red bars) on HER2-expressing SKOV-3 (A and B) and BT474M1 (C and D) cells. Internalized activity (A and C) and total cell-associated activity (B and D), both expressed as percentage of initially cell-bound activity, are shown.

Author Manuscript Author Manuscript Author Manuscript Author Manuscript

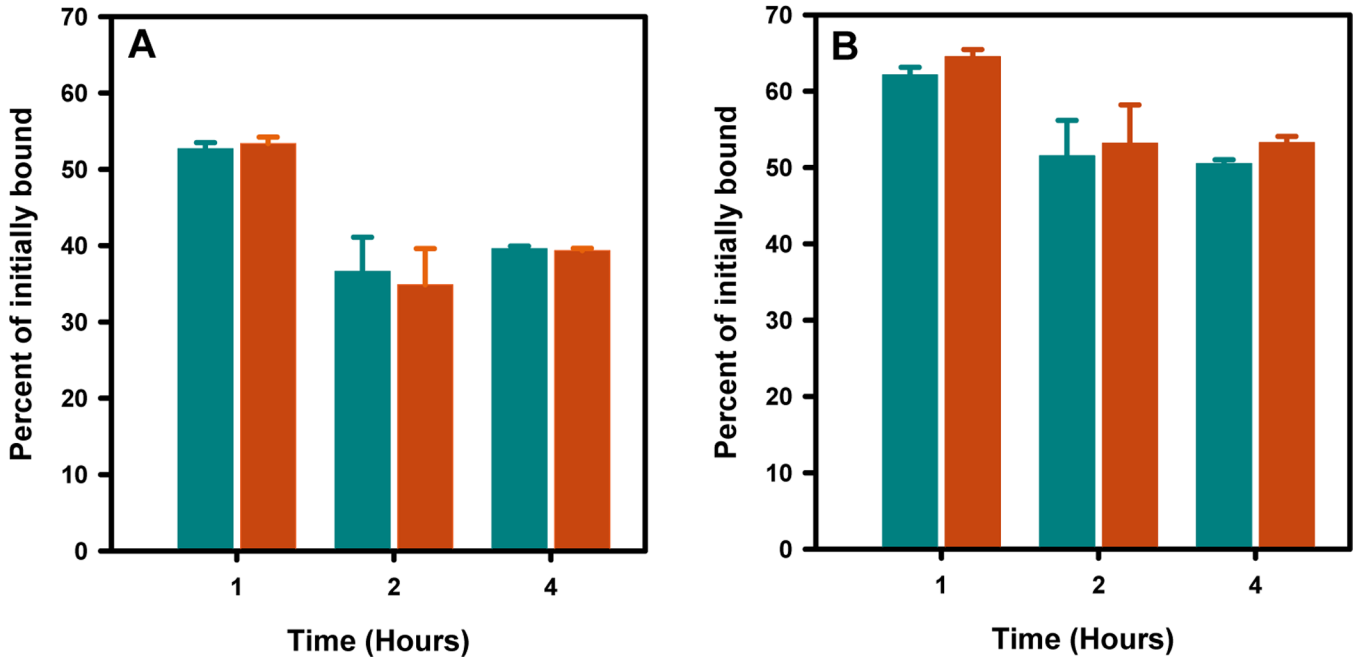

Figure 3.

Paired label internalization of [^{18}F]TFPFN-5F7 (green bars) and *iso*-[^{125}I]SGMIB-5F7 (red bars) on HER2-expressing BT474M1 cells. A) Internalized activity and B) total cell-associated activity both expressed as percentage of initially cell-bound radioactivity.

Author Manuscript Author Manuscript Author Manuscript Author Manuscript

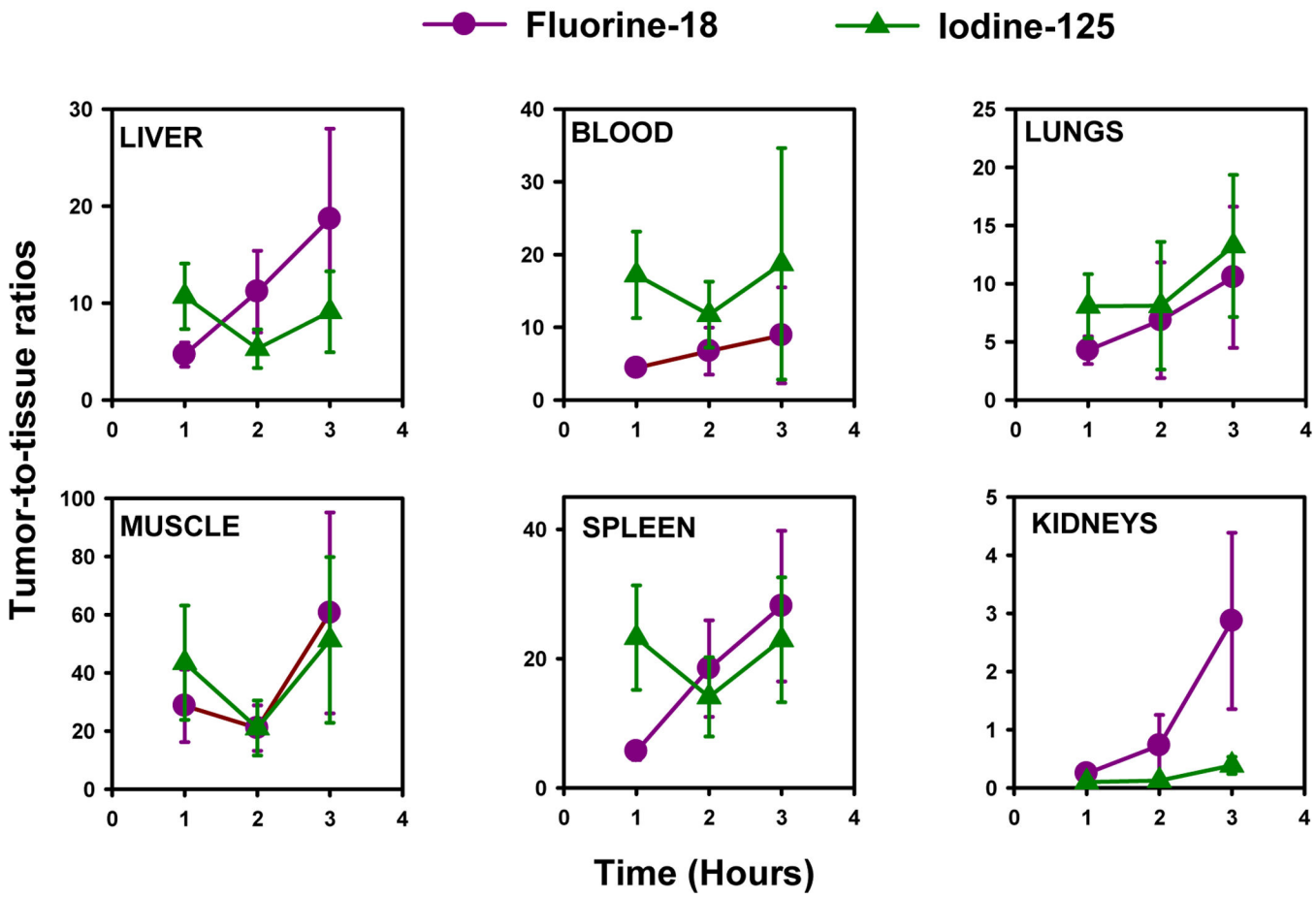

Figure 4.

Tumor-to-normal tissue ratios after injection of [^{18}F]TFPSFN-2Rs15d (magenta) and [^{125}I]SGMIB-2Rs15d (green) in athymic mice with subcutaneous SKOV-3 xenografts.

Author Manuscript Author Manuscript Author Manuscript Author Manuscript

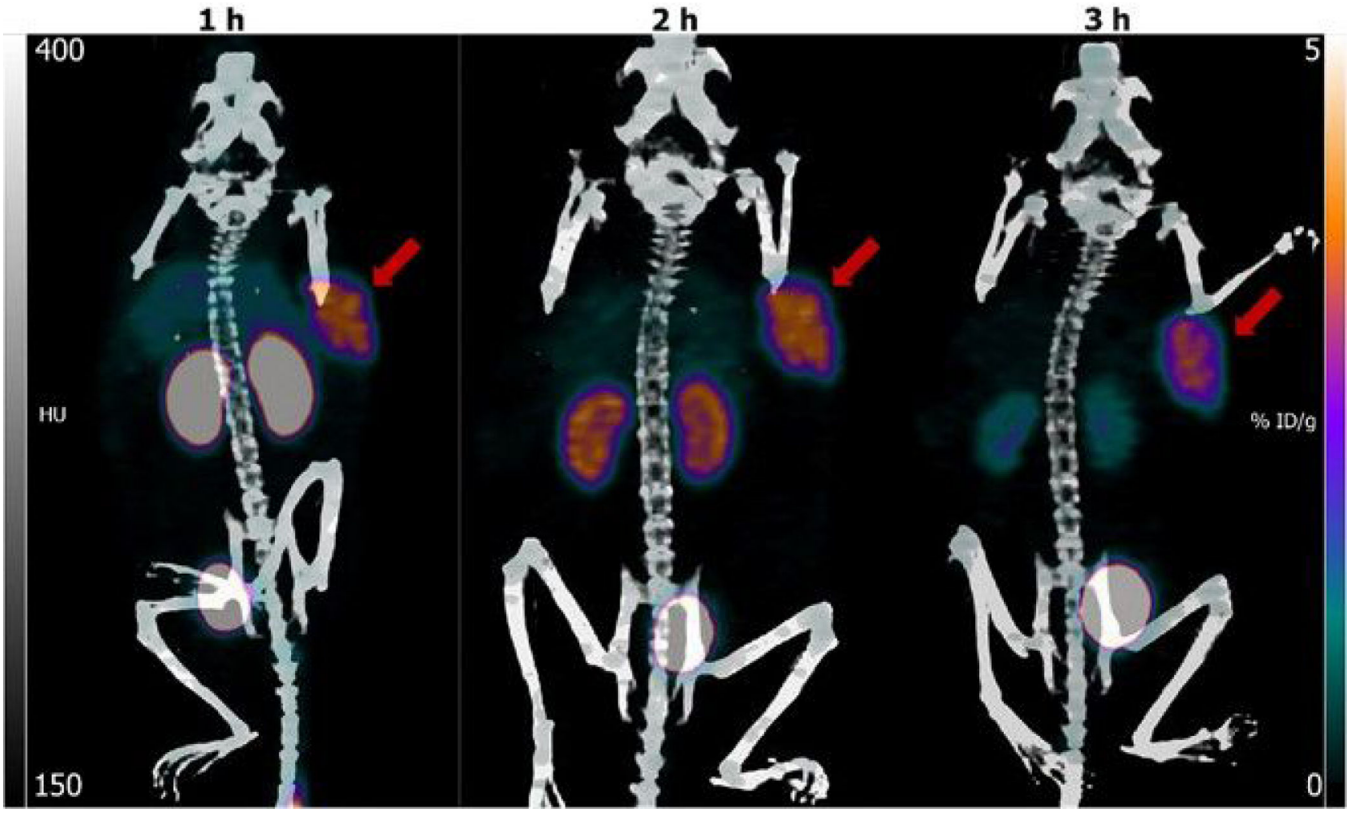

Figure 5.
Maximum intensity projection images obtained 1 h, 2 h and 3 h after injection of [^{18}F]TFPFN-2Rs15d in athymic mouse bearing SKOV-3 xenograft. Tumor indicated by arrow.

Author Manuscript Author Manuscript Author Manuscript Author Manuscript

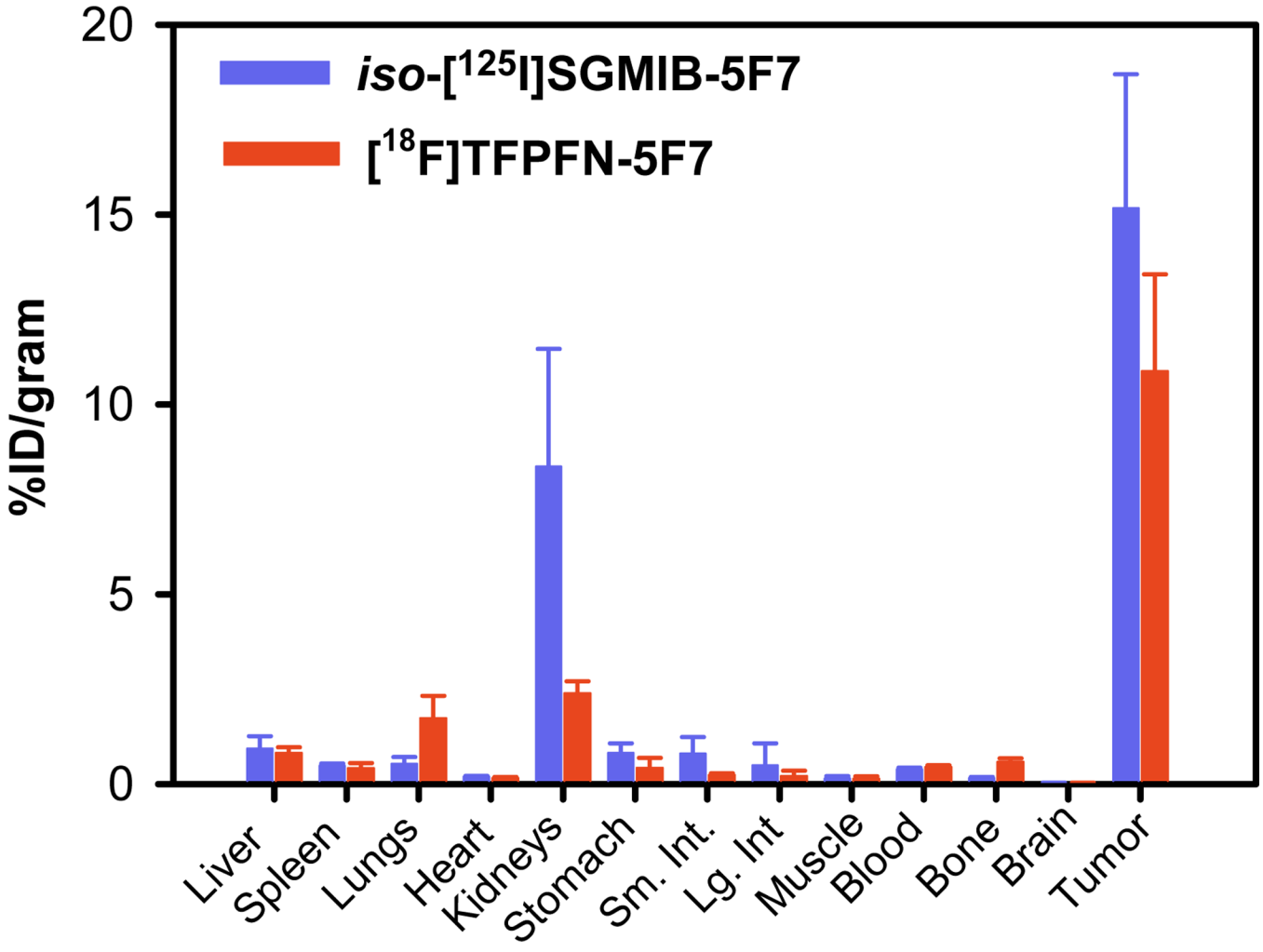

Figure 6.
Paired label biodistribution in athymic mice bearing BT474 xenografts 2 h after administration of *iso*-[^{125}I]SGMIB-5F7 and [^{18}F]TFPFN-5F7.

Author Manuscript Author Manuscript Author Manuscript Author Manuscript

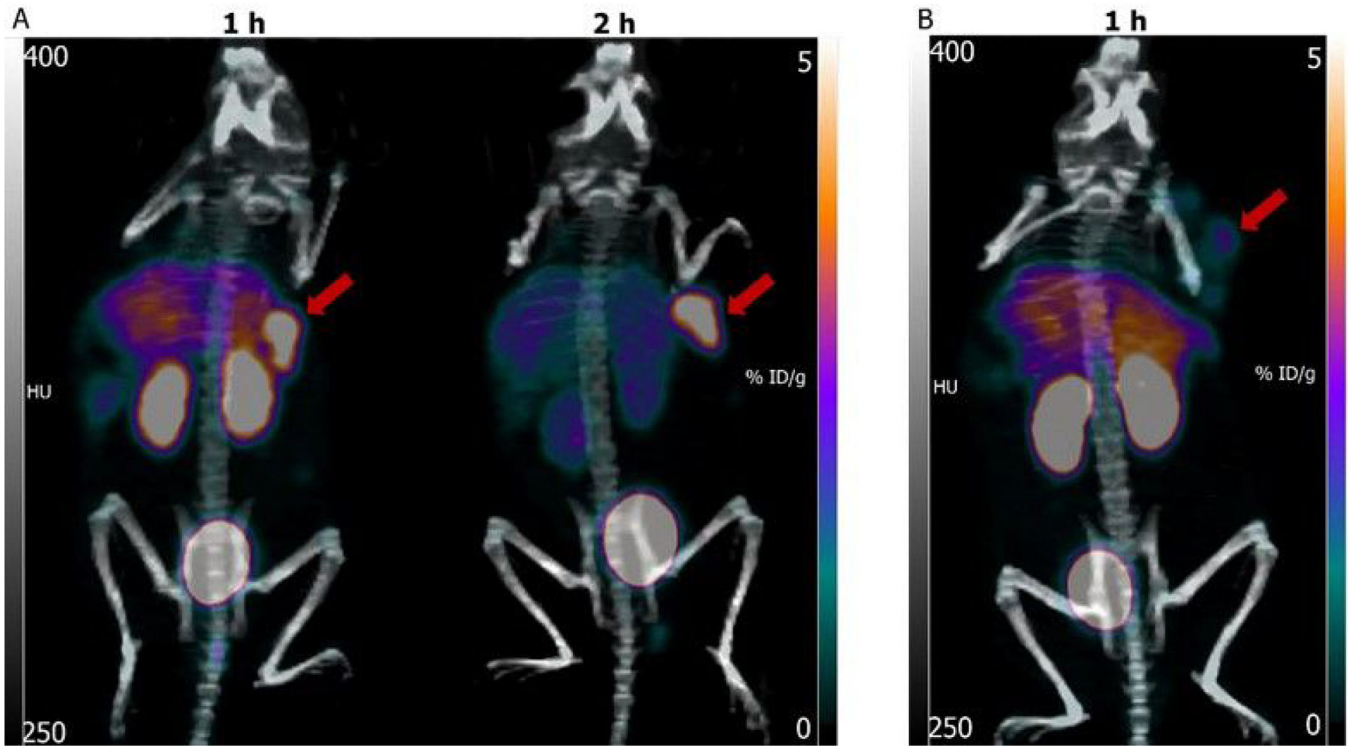

Figure 7.

Maximum intensity projection images obtained after administration of [^{18}F]TFPFN-5F7 in athymic mice bearing SKOV-3 xenografts. A) Representative images of mice 1 h and 2 h after administration of [^{18}F]TFPFN-5F7. B) Image of a mouse (1 h) that received an intravenous blocking dose of trastuzumab 24 h prior to injection of [^{18}F]TFPFN-5F7. Tumors are indicated by arrows.

Author Manuscript Author Manuscript Author Manuscript Author Manuscript

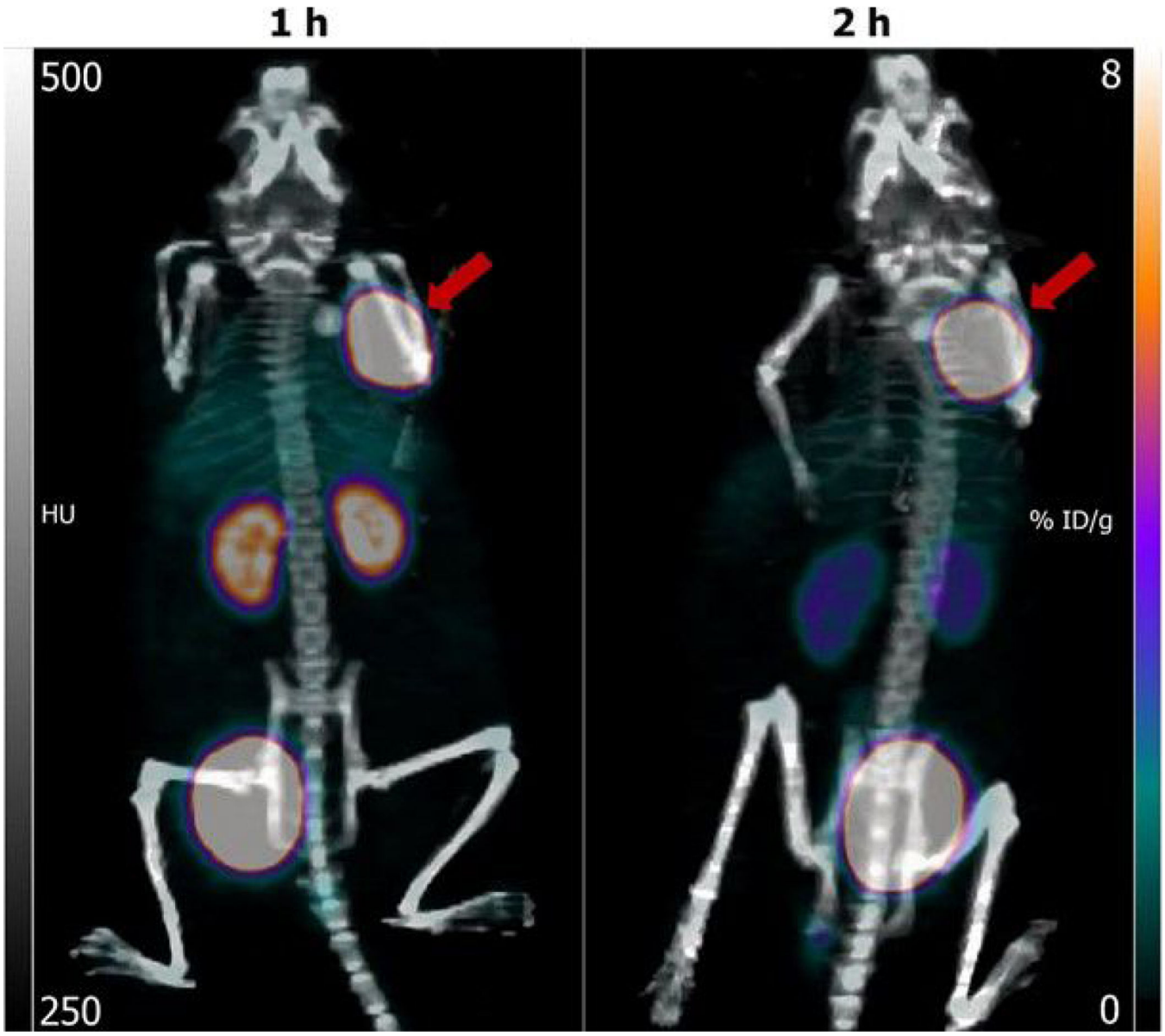

Figure 8.

Typical maximum intensity projection images obtained 1 h and 2 h after injection of [^{18}F]TFPFN-5F7 in athymic mice bearing BT474 xenografts. Tumors are indicated by arrows.

Author Manuscript Author Manuscript Author Manuscript Author Manuscript

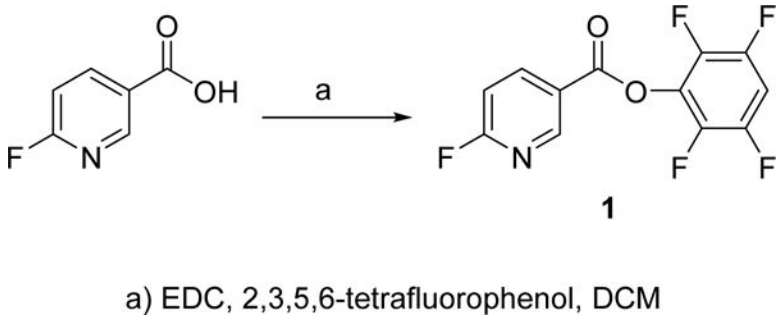

Scheme 1.
Synthesis of and 2,3,5,6-tetrafluorophenyl 6-fluoronicotinate

Author Manuscript Author Manuscript Author Manuscript Author Manuscript

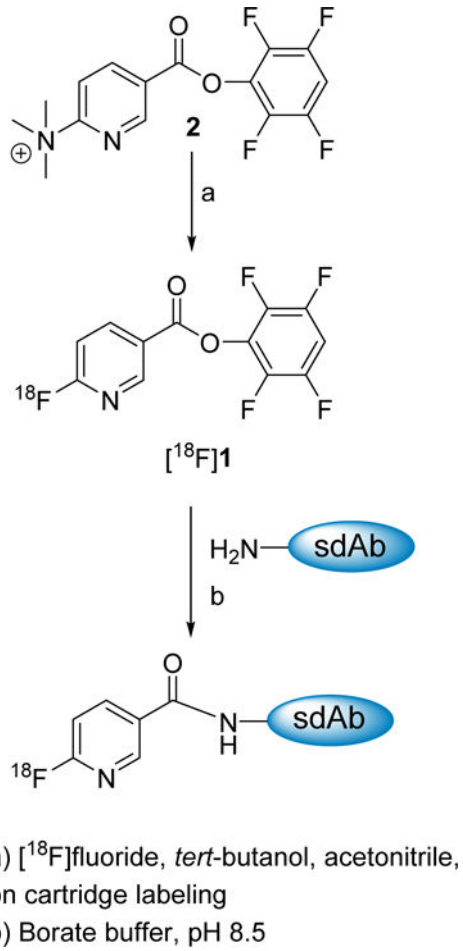

Scheme 2.
Synthesis of 2,3,5,6-tetrafluorophenyl 6-[^{18}F]fluoronicotinate and conjugation to sdAb

Author Manuscript Author Manuscript Author Manuscript Author Manuscript

Table 1.

Paired-label biodistribution of [^{18}F]TFPFN-2Rs15d and [^{125}I]SGMIB-2Rs15d in athymic mice bearing SKOV-3 xenografts.

Tissue	Percent injected dose per gram[a]					
	1 h		2 h		3 h	
	^{125}I	^{18}F	^{125}I	^{18}F	^{125}I	^{18}F
Liver	0.36 ± 0.06	0.81 ± 0.18	0.64 ± 0.18	0.27 ± 0.07	0.39 ± 0.02	0.16 ± 0.01
Spleen	0.17 ± 0.03	0.69 ± 0.29	0.24 ± 0.05	0.17 ± 0.03	0.15 ± 0.02	0.10 ± 0.03[c]
Lungs	0.49 ± 0.12	0.89 ± 0.26	0.74 ± 0.76	1.15 ± 1.49[c]	0.27 ± 0.07	0.28 ± 0.04[c]
Heart	0.16 ± 0.03	0.29 ± 0.06	0.20 ± 0.08	0.15 ± 0.08	0.12 ± 0.02	0.11 ± 0.04[c]
Kidneys	39.04 ± 5.87	15.82 ± 3.88	30.16 ± 11.68	6.62 ± 5.83	9.01 ± 3.06	1.05 ± 0.45
Stomach	0.45 ± 0.19	0.17 ± 0.13	2.04 ± 0.79	0.72 ± 0.35	0.62 ± 0.57	0.08 ± 0.03[c]
Sm. Int.	0.26 ± 0.12	0.19 ± 0.04[c]	0.57 ± 0.20	0.16 ± 0.06	0.14 ± 0.04	0.05 ± 0.01
Lg. Int.	0.10 ± 0.03	0.13 ± 0.03[c]	0.38 ± 0.30	0.13 ± 0.07[c]	0.32 ± 0.34	0.08 ± 0.04[c]
Muscle	0.10 ± 0.04	0.16 ± 0.08[c]	0.17 ± 0.04	0.14 ± 0.03[c]	0.07 ± 0.02	0.05 ± 0.01[c]
Blood	0.23 ± 0.03	0.84 ± 0.10	0.28 ± 0.04	0.49 ± 0.16	0.36 ± 0.42	0.43 ± 0.30[c]
Bone	0.15 ± 0.07	0.32 ± 0.08[b]	0.19 ± 0.13	0.39 ± 0.13	0.11 ± 0.03	0.29 ± 0.17
Brain	0.02 ± 0.01	0.05 ± 0.02	0.03 ± 0.01	0.03 ± 0.01[c]	0.01 ± 0.00	0.02 ± 0.00
Tumor	3.87 ± 1.35	3.73 ± 1.14[c]	3.30 ± 1.26	2.94 ± 0.94[c]	3.56 ± 1.73	2.92 ± 1.44[c]

[a] %ID/gram, Mean ± SD (n=5 at 1 h; n=4 at 2 h and 3 h)

[b] n = 4

[c] Difference in the uptake between the two tracers statistically NOT significant.